



HAL
open science

Exome sequencing of ATP1A3-negative cases of alternating hemiplegia of childhood reveals SCN2A as a novel causative gene

Eleni Panagiotakaki, Francesco Tiziano, Mohamad Mikati, Lisanne Vijfhuizen, Sophie Nicole, Gaetan Lesca, Emanuela Abiusi, Agnese Novelli, Lorena Di Pietro, Aster Harder, et al.

► To cite this version:

Eleni Panagiotakaki, Francesco Tiziano, Mohamad Mikati, Lisanne Vijfhuizen, Sophie Nicole, et al.. Exome sequencing of ATP1A3-negative cases of alternating hemiplegia of childhood reveals SCN2A as a novel causative gene. *European Journal of Human Genetics*, In press, 32 (2), pp.224-231. 10.1038/s41431-023-01489-4 . hal-04382771

HAL Id: hal-04382771

<https://hal.science/hal-04382771>

Submitted on 12 Jan 2024

HAL is a multi-disciplinary open access archive for the deposit and dissemination of scientific research documents, whether they are published or not. The documents may come from teaching and research institutions in France or abroad, or from public or private research centers.

L'archive ouverte pluridisciplinaire **HAL**, est destinée au dépôt et à la diffusion de documents scientifiques de niveau recherche, publiés ou non, émanant des établissements d'enseignement et de recherche français ou étrangers, des laboratoires publics ou privés.

Exome sequencing of *ATP1A3*-negative cases of alternating hemiplegia of childhood reveals *SCN2A* as a novel causative gene

Eleni Panagiotakaki^{1*}, Francesco D. Tiziano^{2*}, Mohamad A. Mikati^{3*}, Lisanne S. Vijfhuizen⁴, Sophie Nicole⁵, Gaetan Lesca⁶, Emanuela Abiusi⁷, Agnese Novelli⁸, Lorena Di Pietro^{2,7}, I.B.AHC Consortium⁸, IAHCRC Consortium⁹, Aster V.E. Harder^{4,10}, Nicole M. Walley¹¹, Elisa De Grandis^{12,13}, Anne-Lise Poulat¹⁴, Vincent Des Portes¹⁴, Anne Lépine¹⁵, Marie-Cecile Nassogne^{16,17}, Alexis Arzimanoglou^{1,18}, Rosaria Vavassori^{8,9,19}, Jan Koenderink²⁰, Christopher H. Thompson²¹, Alfred L. George, Jr.²¹, Fiorella Gurrieri^{22,23}, Arn M.J.M. van den Maagdenberg^{4,10**}, Erin L. Heinzen^{24,25**}

¹Department of Paediatric Clinical Epileptology, Sleep Disorders and Functional Neurology, Member of the ERN EpiCare, University Hospitals of Lyon (HCL), Lyon, France

²Institute of Genomic Medicine, Catholic University and Policlinico Gemelli, Fondazione Policlinico Universitario Agostino Gemelli IRCSS, Rome, Italy

³Division of Pediatric Neurology and Developmental Medicine, Duke University, Durham, NC, USA

⁴Department of Human Genetics, Leiden University Medical Center, Leiden, The Netherlands

⁵Institute of Functional Genomics, University of Montpellier, CNRS, INSERM, Montpellier, France

⁶Department of Medical Genetics, University Hospital of Lyon and Claude Bernard Lyon I University, Lyon France - Pathophysiology and Genetics of Neuron and Muscle (PNMG), UCBL, CNRS UMR5261 - INSERM U1315, Lyon, France

⁷Department of Life Sciences and Public Health, Section of Genomic Medicine, Università Cattolica del Sacro Cuore, Roma, Italy

⁸ I.B.AHC Consortium - A list of members and their affiliations appears in Supplementary Text

⁹ International Alternating Hemiplegia of Childhood Research Consortium (IAHCRC) A list of members and their affiliations appears in Supplementary Text

¹⁰Department of Neurology, Leiden University Medical Center, Leiden, The Netherlands

¹¹ Division of Medical Genetics, Department of Pediatrics, Duke Health, Durham, NC, USA

¹²Department of Neuroscience, Rehabilitation, Ophthalmology, Genetics, Maternal and Child Health, University of Genoa, Genoa, Italy

¹³Child Neuropsychiatry Unit, IRCCS Istituto Giannina Gaslini, Genova, Italy

¹⁴Pediatric Neurology Department, Member of the ERN EpiCARE, University Hospitals of Lyon (HCL), Lyon, France

¹⁵Service de neuropédiatrie, Centre hospitalo universitaire de la Timone, Marseille, France

¹⁶Institut des Maladies Rares, Cliniques Universitaires Saint-Luc, UCLouvain, Brussels, Belgium

¹⁷Service de Neurologie Pédiatrique, Member of the ERN MetabERN, Cliniques Universitaires Saint-Luc, UCLouvain, Brussels, Belgium

¹⁸Department of Child Neurology and Epilepsy Research Unit, Member of the ERN EpiCARE, Hospital San Juan de Dios, Barcelona, Spain

¹⁹Euro-Mediterranean Institute for Science and Technology I.E.ME.S.T. – Palermo, Italy

²⁰Department of Pharmacology and Toxicology, Radboud University Medical Center, Nijmegen, The Netherlands.

²¹Department of Pharmacology, Northwestern University Feinberg School of Medicine, Chicago, IL, USA

²²Research Unit of Medical Genetics, Department of Medicine, Università Campus Bio-Medico di Roma, Roma, Italy

²³Operative Research Unit of Medical Genetics Fondazione Policlinico Universitario Campus Bio-Medico, Roma, Italy

²⁴Division of Pharmacology and Experimental Therapeutics, Eshelman School of Pharmacy, University of North Carolina at Chapel Hill, Chapel Hill, NC, USA

²⁵Department of Genetics, School of Medicine, University of North Carolina at Chapel Hill, Chapel Hill, NC, USA

*/**These authors contributed equally to this work

Running title: Genetics of ATP1A3-negative AHC

Corresponding Authors:

Erin L. Heinzen, PharmD, PhD; Division of Pharmacotherapy and Experimental Therapeutics in the Eshelman School of Pharmacy and Department of Genetics in the School of Medicine, University of North Carolina at Chapel Hill, Chapel Hill, NC, USA; E-mail: eheinzen@unc.edu; Arn M.J.M. van den Maagdenberg, PhD; Department of Human

Genetics, Leiden University Medical Center, Leiden, the Netherlands; E-mail:
A.M.J.M.van_den_Maagdenberg@lumc.nl

Date 31-07-2023

Suggested journal: *European Journal of Human Genetics* Type: Original study

Paper format requirements

Title	120
Abstract	246
Main body of text	3580
References	30
Figures/Tables	2 tables, 3 figures

Abstract

Alternating hemiplegia of childhood (AHC) is a rare neurodevelopment disorder that is typically characterized by debilitating episodic attacks of hemiplegia, seizures, and intellectual disability. Over 85% of individuals with AHC have a *de novo* missense variant in *ATPIA3* encoding the catalytic $\alpha 3$ subunit of neuronal Na^+/K^+ ATPases. The remainder of the patients are genetically unexplained. Here, we used next-generation sequencing to search for the genetic cause of 26 *ATPIA3*-negative index patients with a clinical presentation of AHC or an AHC-like phenotype. Three patients had affected siblings. Using targeted sequencing of exonic, intronic, and flanking regions of *ATPIA3* in 22 of the 26 index patients, we found no ultra-rare variants. Using exome sequencing, we identified the likely genetic diagnosis in 9 probands (35%) in five genes, including *RHOBTB2* ($n = 3$), *ATPIA2* ($n = 3$), *ANK3* ($n = 1$), *SCN2A* ($n = 1$), and *CHD2* ($n = 1$). In follow-up investigations, two additional *ATPIA3*-negative individuals were found to have rare missense *SCN2A* variants, including one *de novo* likely pathogenic variant and one likely pathogenic variant for which inheritance could not be determined. Functional evaluation of the variants identified in *SCN2A* and *ATPIA2* supports the pathogenicity of the identified variants. Our data show that genetic variants in various neurodevelopmental genes, including *SCN2A*, lead to AHC or AHC-like presentation. Still, the majority of *ATPIA3*-negative AHC or AHC-like patients remain unexplained, suggesting that other mutational mechanisms may account for the phenotype or that cases may be explained by oligo- or polygenic risk factors.

Key words: alternating hemiplegia of childhood, AHC, exome sequencing, genetics,
RHOBTB2, SCN2A

Introduction

Alternating hemiplegia of childhood (AHC) is a rare, early-onset neurodevelopmental disorder with a distinctive clinical presentation, first described in 1971, that involves episodic hemiplegia that can affect alternately both sides of the body [1]. These individuals may also have episodes of quadriplegia, paroxysmal attacks of dystonia, abnormal eye movements, and/or autonomic dysfunction, and movement disorders such as chorea, dystonia, and intellectual disability [1-5]. In 2012, *de novo* variants in *ATPIA3* were found to explain the vast majority (~85%) of cases of AHC, providing evidence of the early clinical hypotheses that suggested a distinct monogenic phenotype [6,7]. Still, a number of patients who fulfill the clinical diagnostic criteria of AHC remain genetically unexplained. As comprehensive sequencing of the coding regions of *ATPIA3* had not identified a causal mutation, these cases are referred to as *ATPIA3*-negative, either typical AHC patients or patients with one or more of the hallmark clinical traits observed in the condition (AHC-like). Exome sequencing in parallel studies has shown that rare protein-disrupting variants in *ATPIA2* [8,9] and *RHOBTB2* [10,11] contribute to AHC, although these collectively explain a very small fraction of cases. Hence we here sought to (1) use targeted whole-gene sequencing of *ATPIA3* to look for non-coding pathogenic variants in our cohort of 26 *ATPIA3*-negative patients, and (2) use exome sequencing to further identify other genes that may be responsible for the observed phenotypes.

Materials (Subjects) and Methods

Study participants

Twenty-six individuals with typical AHC (or AHC-like) were consented and enrolled at either Duke University, University Hospitals of Lyon, Catholic University in Rome, or Leiden University Medical Center. Unaffected parents were also collected for 20 of the probands (Table 1). Seventeen probands were sporadic, one proband had two additional affected full siblings (quintet), one proband had one affected sibling (quad), and one proband had an affected half-sibling (Fig. 1). Probands were classified as “typical” if they fulfilled the diagnostic criteria [2]. In all cases, only one affected child underwent targeted gene or exome sequencing. DNA was extracted from blood or saliva from the proband and unaffected parents for genomic analyses at the referral Centers. Our control cohort consisted of 11,151 individuals sequenced as part of other genetics studies in the Institute for Genomic Medicine (Columbia University, New York, NY, USA) was used to exclude site-specific artifacts and ascertain variant frequency in the population. This cohort consisted of healthy individuals or individuals with phenotypes unrelated to neurodevelopmental disorders.

Following the analysis of the exome sequence data, two additional *ATPIA3*-negative AHC cases (IT06 and 13A2344) were identified with rare missense *SCN2A* variants. These individuals were sequenced and analyzed as part of other studies. Since they were not analyzed as part of the initial cohort, these are being reported as secondary findings. Phenotypic information based on presence or absence of the six core features of AHC[2] is provided for all probands and affected family members ($n = 32$) (Supplementary Table 1).

Targeted and exome sequencing and data processing

DNA samples from all 26 probands and parents underwent exome sequencing using either the IDT xGen Exome Research Panel v1 (IDT Corporation, Newark, New Jersey, USA) or the Nimblegen SeqCap EZ V3.0 Exome Enrichment Kit (NimbleGen Systems GmbH, Pleiskirchen, Germany) per protocol. A subset of 22 probands also underwent targeted sequencing on a custom-designed panel (Nimblegen SeqCap EZ V3.0 Custom Enrichment Kit; NimbleGen Systems GmbH, Pleiskirchen, Germany) that included the full gene sequence of *ATPIA3*, including protein-coding, non-coding, and 1 kb up- and downstream of the protein-coding sequence. The other four samples from the exome-sequenced cohort did not have sufficient DNA available for such targeted deep sequencing of *ATPIA3*. Sequencing was performed on the HiSeq2500 and NovaSeq platforms (Illumina, Inc., San Diego, CA, USA). The sequenced fragments were aligned with DRAGEN to hg19/ GRCh37. Variants were called using the Genome Analysis Toolkit (GATK) v3.6 best practices [12]. Variants were annotated using consensus coding sequence (release 20) using snpEff [13]. Genomic analyses were performed using Analysis Tool for Annotated Variants (ATAV) [14].

Two additional cases with an *SCN2A* variant were identified separately from the 26 exome-sequenced probands. One case harboring the *de novo* variant in *SCN2A* underwent exome sequencing at Catholic University in Rome using the Ion AmpliSeq™ Exome RDY Kit (Thermo Fisher Scientific, Waltham, MA, USA) according to the manufacturer's instructions. Sequencing was performed by the ION-Proton Instrument (Thermo Fisher Scientific, Waltham, MA, USA). Raw data were aligned to the hg19 by the Torrent Suite (v.5.0.4). Following the upload of the BAM file into the Ionreporter cloud tool, variants were identified by the Variant Caller Plugin (v. 5.10). The second individual, who was found to

have an *SCN2A* variant, underwent targeted sequencing using a custom Nimblegen SeqCap EZ V3.0 Custom Enrichment Kit targeted (NimbleGen Systems GmbH, Pleiskirchen, Germany) that included the protein-coding regions of *SCN2A*. Parental DNA was unavailable in this case to ascertain inheritance.

Calling of rare variants and genotypes from exome and target sequencing in probands

De novo variants were identified from the annotated variant lists using the following criteria:

(1) heterozygous variant call in the proband with at least 10-fold coverage; (2) exclude variants with a minor allele frequency (MAF) >0% in the Institute of Genomic Medicine control cohort, and in Exome Variant Server (EVS), Exome Aggregate Consortium (ExAC release 0.3), and gnomAD browser (v2.1.1); (3) exclude variants with a GATK RMSMappingQuality score of <40, QualbyDepth Score <2, quality score <50; (4) exclude variants with a variant allele fraction of <30% and <70%; (5) exclude variants in RepeatMasker regions (RepeatMasker 4.1.0, <http://www.repeatmasker.org>); (6) in cases where sequencing of unaffected was performed, the parents were required to have a homozygous reference genotype with at least 10-fold coverage; and (7) for exome sequence analysis, we further limited *de novo* variant calls only to those predicted to modify the function or amount of protein [missense (PolyPhen2 probably/possibly damaging), variants in conserved splicing regions (variant at the exon-intron boundary within 3 bases into an exon or 8 bases into the intron), nonsense, or indels]. Given the high rate of false positives when the variant allele fractions were <30%, we only evaluated known pathogenic variants and any variant in *ATPIA3* with variant allele fractions to consider the possibility of

mosaicism for the gene-negative AHC cases. The list of *de novo* variants is provided in Supplementary Table 2.

We also compiled rare hemizygous and homozygous genotypes from each of the probands using the following criteria: (1) homozygous or hemizygous genotype in the proband with at least 10-fold coverage; (2) exclude genotypes at variant sites with MAF <0.5% in any population subset and homozygous and/or hemizygous genotype frequency >0 among internal controls or any population in Exome Variant Server (EVS), Exome Aggregate Consortium (ExAC release 0.3), and gnomAD browser (v2.1.1)]; (3) exclude variants with a GATK RMSMappingQuality score of <40 and a GQ score of <20 in the proband; (4) exclude genotypes in the proband with a variant allele fraction of <80%; (5) exclude variants in RepeatMasker regions; (6) in cases where sequencing of unaffected was performed, both parents were required to have 10-fold coverage at the variant site and the mother was required to be heterozygous for hemizygous candidates in the proband, and both mother and father were required to be heterozygous for homozygous candidates in the proband parents were required to have a heterozygous genotype; and (7), for exome sequence analysis, we further limited homozygous and hemizygous variant calls only to those predicted to modify the function or amount of protein [missense (PolyPhen2 probably/possibly damaging), variants in conserved splicing regions (variant at the exon-intron boundary within 3 bases into an exon or 8 bases into the intron), nonsense, or indels]. The list of candidate homozygous and hemizygous genotypes in the probands is provided in Supplementary Table 2.

Finally, compound heterozygous genotypes from the proband were compiled by first compiling all qualifying heterozygous variant calls that included (1) heterozygous variant call in the proband with at least 10-fold coverage; (2) exclude variants with minor allele

frequency >0.5% in the Institute of Genomic Medicine control cohort, and in Exome Variant Server (EVS), Exome Aggregate Consortium (ExAC release 0.3), and gnomAD browser (v2.1.1); (3) exclude variants with a GATK RMSMappingQuality score of <40, QualbyDepth Score <2, quality score <50; (4) exclude variants with a variant allele fraction of <30% and <70%; (5) exclude variants in RepeatMasker regions; and (6), for exome sequence analysis, we further limited candidate *de novo* variant calls only to those predicted modify the function or amount of protein [missense (PolyPhen2 probably/possibly damaging), variants in conserved splicing regions (variant at the exon-intron boundary within 3 bases into an exon or 8 bases into the intron), nonsense, or indels].

Compound heterozygous genotypes were only evaluated in trios where we could confirm bi-allelic inheritance. The list of compound heterozygotes in the probands is provided in Supplementary Table 2.

Variants were assessed for pathogenicity using the principles outlined by the American College of Medical Genetics (ACMG) [15].

Functional evaluation of *ATPIA2* variants

Human Na⁺/K⁺-ATPase α 2 subunit cDNA was subcloned as previously described [16]. In brief, to distinguish endogenous Na⁺/K⁺-ATPase activity from that of transfected Na⁺/K⁺-ATPase, two additional mutations were introduced in the original α 2 subunit cDNA to express an ouabain-resistant isoform. Next, FHM2 missense variants p.E332Q and p.M813K were introduced into the ouabain-resistant wild-type α 2 subunit construct by site-directed mutagenesis. All constructs were sequence verified.

HeLa cells (5×10^5) were transfected with 1.6 μg plasmid DNA using Lipofectamine 2000 Transfection Reagent in Opti-Mem medium (Invitrogen, Waltham, MA, USA) and cultured in DMEM-containing Glutamax and 10% FCS. Two days after transfection, one-third of the cells were seeded on 10-cm petri dishes and after 5 days of ouabain (1 μM) challenge, colonies were stained with 1% methylene blue in 70% methanol, scanned, and analyzed with ImageJ ((NIH and LOCI, University of Wisconsin, WI, USA). Each transfection was performed three times in triplicates. Two days after transfection, two-thirds of the cells were harvested for Western blot analysis as described previously [16]. The $\alpha 2$ subunit-specific polyclonal antibody HERED was used for staining [17]. The blot was incubated with the secondary antibody goat anti-rabbit Alexa Fluor™ 680 (Abcam, Cambridge, UK) and scanned, with the Odyssey Imaging System (LI-COR Biosciences, Lincoln, NE, USA).

Functional evaluation of *SCN2A* variants

HEK293T cells stably transfected with the human sodium channel $\beta 1$ (*SCN1B*) and $\beta 2$ (*SCN2B*) auxiliary subunits (HEK-beta cells) were maintained in Dulbecco's modified Eagle's medium (GIBCO/Invitrogen, San Diego, CA, USA) supplemented with 10% fetal bovine serum (Atlanta Biologicals, Norcross, GA, USA), 2 mM L-glutamine, 50 units/mL penicillin, and 50 $\mu\text{g}/\text{mL}$ streptomycin at 37°C in 5% CO₂. For automated electrophysiology experiments, full-length WT or variant *SCN2A* (Nav1.2) cDNA was electroporated into HEK-beta cells using the MaxCyte STX electroporation system (MaxCyte Inc., Gaithersburg, MD, USA). Automated patch clamp recording was performed using the

Nanion Sycropatch 768PE platform (Nanion Technologies, Munich, Germany) using single-hole low resistance (3-4 M Ω) recording chips. Pulse generation and data collection were performed using PatchControl384 v1.6.6 and DataControl384 v1.6.0 software (Nanion Technologies, Munich, Germany). Whole-cell currents were acquired at 10 kHz, series resistance was compensated 80%, and leak currents were subtracted using P/4 subtraction. The external solution contained (in mM): 140 NaCl, 4 KCl, 2 CaCl₂, 1 MgCl₂, 1 HEPES, 5 glucose, with the final pH adjusted to 7.4 with NaOH, and osmolality adjusted to 300 mOsm/kg/L with sucrose. The composition of the internal solution was (in mM): 110 CsF, 10 CsCl, 10 NaCl, 20 EGTA, 10 HEPES, with the final pH adjusted to 7.2 with CsOH, and osmolality adjusted to 300 mOsm/kg/L with sucrose. High-resistance seals were obtained by addition of seal enhancer solutions, which was comprised of (in mM): 80 NaCl, 3 KCl, 35 CaCl₂, 10 MgCl₂, 10 HEPES, with the final pH adjusted to 7.4 with NaOH. Prior to recording, cells were washed twice with external solution, and the final concentrations of CaCl₂ and MgCl₂ were 3 mM and 2 mM, respectively. Biophysical data were collected only from cells with currents larger than -200 pA. Stringent criteria were set to select cells included in the final analysis (seal resistance ≥ 200 M Ω , access resistance ≤ 20 M Ω , capacitance ≥ 2 pF, and sodium reversal potential between 45 and 85 mV. Voltage control was assessed from conductance-voltage (GV) curves and cells were included in the final analysis if two adjacent points on the GV curve showed no more than a 7-fold increase. Unless otherwise noted, all chemicals were obtained from SigmaAldrich (St. Louis, MO, USA). Data were analyzed and plotted using a combination of DataControl384 v1.6.0 (Nanion Technologies, Munich, Germany), Clampfit 10.4 (Molecular Devices, San Jose, CA, USA), Microsoft Excel

(Microsoft Office 2019, Remond, WA, USA), and GraphPad Prism (GraphPad Software, San Diego, CA, USA). Whole-cell currents were normalized to membrane capacitance, and data are expressed as mean \pm SEM unless otherwise noted. One-way ANOVA with Dunn's *post hoc* test was used for statistical comparison, and the threshold for statistical significance was $P \leq 0.05$.

Results

Analysis of *ATP1A3*

The protein-coding sequencing from both targeted and exome sequencing of *ATP1A3* in the 26 probands was nearly complete with 98% of protein-coding exons sequenced at least 10-fold on average (min. 96%) (Table 1). Across any of the 22 individuals undergoing targeted sequencing, we identified no mosaic or germline *de novo* variants in protein-coding or non-coding regions in leukocyte-derived DNA. We also found no homozygous or compound heterozygous variants in any of the cases.

Exome sequence analysis

De novo variants

A total of 31 protein-coding putatively functional *de novo* variants were identified in the 20 trios who underwent exome sequencing. Only one gene, *RHOBTB2*, had *de novo* variants in multiple individuals with three individuals having three different missense variants. Observing three *de novo* variants in three different individuals accounting for gene size, sequence mutability is highly unlikely to occur by chance (FitDNM, $P = 1.3 \times 10^{-11}$) [18]. Even correcting for the ~18K genes using a Bonferroni correction, the enrichment is still significant.

American College of Medical Genetics and Genomics (ACMG) diagnostic analysis

In addition to the three likely pathogenic variants in *RHOBTB2*, we also identified pathogenic or likely pathogenic *de novo* variants in additional probands in *ATPIA2* ($n = 1$), *ANK3* ($n = 1$), *CHD2* ($n = 1$), and *SCN2A* ($n = 1$). The *de novo* variant in *CHD2* was identified in a family with two affected children, however, the other affected child did not carry the *CHD2* variant. Clinically, the *CHD2* variant was deemed to be pathogenic and partially contributing to the phenotype of the proband. Overall, no pathogenic or likely pathogenic compound heterozygous variant sets or homozygous or newly hemizygous variants were identified.

One variant of unknown significance was identified in the exome sequence data, a stop-gained variant *RHOBTB2* that was inherited from an unaffected father (Table 2, Supplementary Table 2).

Phenotyping and functional characterization

RHOBTB2: In total, we identified three likely pathogenic variants and one variant of unknown significance (VOUS) in *RHOBTB2* (Table 2). Two of the cases with a genetic diagnosis presented with typical AHC (ahc13A581ag1ex and ahcahc2k1) while one presented atypically lacking obvious bouts of hemiplegia or quadriplegia (ahcdukeepi4538bh1). The case with the stop gained VOUS (ahcdukeepi4542bv1) also presented atypically with unclear information regarding bouts of hemiplegia or quadriplegia (Supplementary Table 1).

ATPIA2: Among the exome-sequenced cases, we identified three rare variants in *ATPIA2*, including one likely pathogenic *de novo* variant, one likely pathogenic variant with unknown inheritance, and one likely pathogenic splice site variant in *ATPIA2* inherited from

a father who is diagnosed with hemiplegic migraine. Only the likely pathogenic variant with unknown inheritance presented with an atypical presentation with no reports of quadriplegia or relief from hemiplegic attacks upon sleeping (ahcdukeepi4542bw1, Supplementary Table 1). None of the three probands were deemed clinically to have hemiplegic migraine (Supplementary Table 1). We note that two of the individuals with likely pathogenic *ATP1A2* variants (ahcdukeepi4542bw1 and ahcdukeepi4524bo1) were reported in a previous publication [19] and reported to have an epileptic encephalopathy in addition to having clinical presentations consistent with AHC. *In vitro* functional evaluation of p.E332Q and p.M813K demonstrated that the expression levels were comparable or higher than that of the wild-type, whereas cell survival was decreased to 14% and 0%, respectively (Fig. 2). This indicates that both variants have functional consequences on sodium–potassium pump functioning and can be considered pathogenic. Consistent with these *in vitro* functional findings, a previous publication reported AHC-like phenotypes in an M813K mouse model [19].

SCN2A: In addition to the identification of the in-frame *de novo* *SCN2A* indel (p.E1493del) in one of the patients included in this study, we had identified (likely) pathogenic rare missense variants (p.E1551G, p.F1651V) in two additional cases that met the AHC criteria prior to the initiation of this study. One of the newly identified *SCN2A* variants was *de novo* and the other was of unknown inheritance (parental samples were not available). *In vitro* functional evaluation of all three variants demonstrated varying patterns of dysfunction (Fig. 2; Supplemental Table 3). The *de novo* *SCN2A* indel variant exhibited current density that was not significantly different from background (endogenous) indicating a complete loss-of-function. By contrast, the two missense variants were functional but had

significantly altered properties including depolarized voltage-dependence of steady-state inactivation, slower time course of fast inactivation, significantly enhanced channel activation during a slowly depolarizing voltage ramp (p.E1551G only), slower recovery from inactivation and greater loss of activity with repeated depolarizations. These functional features support the pathogenicity of the *SCN2A* variants.

Discussion

In this study, we sought to determine the genetic cause of 26 unrelated probands with AHC or an AHC-like phenotype with no molecular diagnosis. Comprehensive (intronic, exonic, and 1-kb flanking regions) and exome sequencing of the *ATPIA3* gene found no evidence of overlooked *ATPIA3* variants. However, likely genetic diagnoses were identified in 11 probands (42%) in five genes, including *RHOBTB2* ($n = 3$), *ATPIA2* ($n = 3$), *ANK3* ($n = 1$), *SCN2A* ($n = 3$), and *CHD2* ($n = 1$). Each of these genes has been previously associated with neurodevelopmental (or neurological) disorders [16, 21], and two (*RHOBTB2* and *ATPIA2*) have been specifically implicated in AHC or AHC-like presentations [9,11,20]. These observations are consistent with several isolated case reports of AHC or AHC-like presentations in individuals with likely pathogenic variants in neurodevelopmental disorder genes not classified as AHC genes (*cf.* Panagiotakaki et al. 2023) [21].

ATPIA2 was first associated in 2004 when a rare variant was found to co-segregate in a large multiplex family with AHC and familial hemiplegic migraine [8]. Mutations in *ATPIA2* are, however, most commonly known to cause hemiplegic migraine type 2 [22], a rare autosomal dominant severe form of migraine with aura [23]. In hemiplegic patients, the aura consists of transient motor weakness varying from mild paresis to hemiplegia. There is

overlap in the phenotypic spectrum between hemiplegic migraine and AHC [8,24] based on clinical similarities of the attacks and the paroxysmal nature of both disorders. A distinction can be made based on choreoathetosis, dystonic posturing, and a progressive course associated with intellectual disability [2,20,25]. Our genetic findings, coupled with functional analyses supporting pathogenicity, further solidify the association of *ATPIA2* in AHC.

RHOBTB2 likewise was previously associated with AHC and AHC-like presentations [11]. In that study [11], 11 affected patients were described all with rare heterozygous missense variants in exon 9; in nine patients it was possible to assess the parent of origin and it was found that the variants had originated *de novo*. Two out of three of the likely pathogenic variants in *RHOBTB2* identified in this study were located in exon 9 (exon 5 of the protein-coding sequence) (Table 2). The majority of our cases had presentations that met the criteria of AHC or had significant phenotypic overlap. An additional case of a rare *de novo* variant in *RHOBTB2* was later reported in another case with an AHC-like presentation [10].

In addition to identifying variants in known genes (*ATPIA2* and *RHOBTB2*), we also identified a rare *de novo* in-frame indel variant in *SCN2A*. While *de novo* *SCN2A* mutations have been reported extensively in neurodevelopmental disorders that sometimes include movement disorders including dystonia and episodic ataxia [2,26,27], we are the first to report a case that meets the AHC diagnostic criteria. Follow-up investigations identified two additional *ATPIA3*-negative typical AHC cases who were found to have a likely pathogenic *SCN2A* *de novo* variant in a parallel sequencing initiative. Even though the parent of origin of the other *SCN2A* variant could not be ascertained, functional data generated in this study support the variant's pathogenicity (Fig. 3).

Despite comprehensive exome sequencing, 65% ($n = 17$) of the cases studied remain genetically unexplained. These cases may be caused by variants not captured by our analyses, including non-coding variants, variants not detectable with short-read next-generation sequencing technology (complex structural rearrangements, short-tandem repeat, and copy number variants), poly- or oligogenic genetic architecture, post-zygotic events undetectable in blood, or possibly phenocopies. Future research is needed to investigate other sources of genetic variation that may explain the outstanding genetically unexplained AHC cases.

Our findings collectively suggest that some individuals with AHC or AHC-like presentations without an *ATPIA3* variant are due to genetic variants in a small number of known neurodevelopmental disease genes that have clinical presentations that have some features associated with AHC. Given the highly variable phenotypic presentation for *ATPIA3* [6,7,25,28,29] and the genetic heterogeneity observed in this study, thorough investigation of *ATPIA3* and other neurodevelopment disease genes in the clinical genetic diagnostic workup in individuals with AHC or clinical features associated with AHC is warranted.

Acknowledgments

We greatly acknowledge the subjects who participated in this study. We also thank Jean-Marc DeKeyser and Tatiana Abramova for generating and expressing the *SCN2A* variants. Moreover, we thank Geert van Weelden and Jeroen van den Heuvel for their help with the functional analysis of the *ATPIA2* variants.

I.B.AHC Consortium - Members

Maria Teresa Bassi, Claudio Zucca – Scientific Institute IRCCS E. Medea, Bosisio Parini (LC); Elisa De Grandis, Michela Stagnaro, Edvige Veneselli – Istituto G. Gaslini, University of Genoa, Genoa; Filippo Franchini – A.I.S.EA Onlus, Milan; Melania Giannotta, Giuseppe Gobbi – IRCCS Istituto delle Scienze Neurologiche di Bologna, Bologna; Tiziana Granata, Nardo Nardocci, Francesca Ragona – IRCCS Foundation Neurological Institute C. Besta, Milan; Fiorella Gurrieri, Giovanni Neri, Francesco Danilo Tiziano – Istituto di Medicina Genomica Università Cattolica del S. Cuore, Rome; Federico Vigevano – Bambino Gesù Children’s Hospital, IRCCS, Rome; Rosaria Vavassori - Euro-Mediterranean Institute for Science and Technology I.E.ME.S.T. – Palermo, Italy.

Conflicts of Interest

ALG serves on a scientific advisory board for Tevard Biosciences, and consults for Praxis Precision Medicines. ALG receives grant funding from Tevard Biosciences, Praxis Precision Medicines, and Neurocrine Biosciences for unrelated work. AMJMvdM received funding from Schedule 1 Therapeutics and Praxis Precision Medicines for unrelated work. The other authors declare no conflicts of interest.

Author Contributions

EP, FDT, MAM, FG, AMJMvdM, and ELH conceived and designed the study. EP, FDT, MAM, AVEH, LSV, FG, AMJMvdM, and ELH drafted or revised the manuscript. EP, FDT, MAM, LV, SN, AVEH, NMW, FG, AMJMvdM, and ELH generated and interpreted sequence data. CHT, ALG, and JK generated and interpreted the functional data. EP, MAM, SN, GL, EA, AN, LDP, NMW, EDG, ALP, VDP, AL, MCN, AA, and RV provided patient

samples, phenotypic data, and interpreted genotype-phenotype correlations. All authors reviewed and approved the final version and agreed to be accountable for all aspects or the work.

Funding

Genetic studies were funded in part by a grant from Cure AHC (ELH)), AFM-Telethon, and AFHA (SN). Functional studies of *SCN2A* were supported by NIH grant NS108874 (ALG). The variant analysis of *SCN2A* Italian patients was supported by AISEA (FG, FDT)

Ethical Approval

All subjects were consented to participate in this research study through protocols approved by local ethics boards.

Data Availability

The individuals did not consent to controlled release of the data into dbGAP or SRA, however, the raw data analyzed in this study are available from the corresponding author on reasonable request.

Supplementary Information

Supplementary Table 1. Clinical phenotypes of study participants.

Supplementary Table 2. Rare variants and genotypes identified in exome-sequenced *ATP1A3*-negative AHC cohort.

Supplementary Table 3. Functional Properties of AHC2-associated *SCN2A* variants.

Figure Legends

Figure 1. Cohort and overview of analysis approach (made with Biorender).

Figure 2. Ouabain-survival assay in transfected HeLa cells. (A) Western blot analysis of HeLa cells transfected with wild-type (WT) or *ATP1A2* variant cDNA. (anti-HERED antibody). (B) Ouabain sensitivity as determined by cell survival of cells transfected with either wild-type or *ATP1A2* cDNA variants. Bars represent cell survival after 5 days of ouabain treatment ($n = 3$). Error bars show standard error of the mean. WT, p.E332Q, and p.M813K, studied variants. The glutamate residue at position 332 is part of the ion-binding pocket of the Na^+/K^+ -ATPase [30]. Structural effects of replacing glutamic acid with glutamine (E332Q) can lead to a minor conformational shift of the amino acid, disrupting the binding pocket resulting in the observed decrease in cell survival. The methionine residue at position 813 is located in the sixth transmembrane domain, close to cation-binding amino acid aspartate 808. Replacement of this amino acid with the positively charged lysine most likely disturbs the binding pocket in such a way that in our assay cell survival is decreased to zero.

Figure 3. Functional properties of AHC2-associated *SCN2A* variants. (A) Average whole-cell sodium currents normalized to peak current of the wild-type (WT) channel. (B) Current-voltage relationships. (C) Voltage-dependence of activation and inactivation. (D) Average normalized whole-cell sodium currents elicited at 0 mV, and summary data showing time-constant of fast inactivation. (E) Average whole-cell ramp currents normalized to wild-

type current and summary data showing charge movement elicited by the voltage ramp. **(F)** Time course of recovery from inactivation. **(G)** Frequency dependent run down of peak current at 20 Hz. All data are expressed as mean \pm SEM with 28 to 120 cells per group for panels A-C,F,G, and 12-42 cells per group for panels D and E. Color coding is shown in panel B. Asterisks indicate $P < 0.05$ for differences between variant and wild-type SCN2A.

References

1. Verret S, Steele JC: Alternating hemiplegia in childhood: a report of eight patients with complicated migraine beginning in infancy. *Pediatrics* 1971; **47**: 675-680.
2. Bourgeois M, Aicardi J, Goutieres F: Alternating hemiplegia of childhood. *J Pediatr* 1993; **122**: 673-679.
3. Mikati MA, Kramer U, Zupanc ML, Shanahan RJ: Alternating hemiplegia of childhood: clinical manifestations and long-term outcome. *Pediatr Neurol* 2000; **23**: 134-141.
4. Sweney MT, Silver K, Gerard-Blanluet M, Pedespan JM, Renault F, Arzimanoglou A *et al*: Alternating hemiplegia of childhood: early characteristics and evolution of a neurodevelopmental syndrome. *Pediatrics* 2009; **123**: e534-541.
5. Panagiotakaki E, Doummar D, Nogue E, Nagot N, Lesca G, Riant F *et al*: Movement disorders in patients with alternating hemiplegia: "Soft" and "stiff" at the same time. *Neurology* 2020; **94**: e1378-e1385.
6. Heinzen EL, Swoboda KJ, Hitomi Y, Gurrieri F, Nicole S, de Vries B *et al*: De novo mutations in ATP1A3 cause alternating hemiplegia of childhood. *Nat Genet* 2012; **44**: 1030-1034.
7. Rosewich H, Thiele H, Ohlenbusch A, Maschke U, Altmuller J, Frommolt P *et al*: Heterozygous de-novo mutations in ATP1A3 in patients with alternating hemiplegia of childhood: a whole-exome sequencing gene-identification study. *Lancet Neurol* 2012; **11**: 764-773.
8. Swoboda KJ, Kanavakis E, Xaidara A, Johnson JE, Leppert MF, Schlesinger-Massart MB *et al*: Alternating hemiplegia of childhood or familial hemiplegic migraine? A novel ATP1A2 mutation. *Ann Neurol* 2004; **55**: 884-887.
9. Huang D, Liu M, Wang H, Zhang B, Zhao D, Ling W *et al*: De novo ATP1A2 variants in two Chinese children with alternating hemiplegia of childhood upgraded the gene-disease relationship and variant classification: a case report. *BMC Med Genomics* 2021; **14**: 95.
10. Defo A, Verloes A, Elenga N: Developmental and epileptic encephalopathy related to a heterozygous variant of the RHOBTB2 gene: A case report from French Guiana. *Mol Genet Genomic Med* 2022; **10**: e1929.
11. Zagaglia S, Steel D, Krithika S, Hernandez-Hernandez L, Custodio HM, Gorman KM *et al*: RHOBTB2 Mutations Expand the Phenotypic Spectrum of Alternating Hemiplegia of Childhood. *Neurology* 2021; **96**: e1539-e1550.

12. DePristo MA, Banks E, Poplin R, Garimella KV, Maguire JR, Hartl C *et al*: A framework for variation discovery and genotyping using next-generation DNA sequencing data. *Nat Genet* 2011; **43**: 491-498.
13. Cingolani P, Platts A, Wang le L, Coon M, Nguyen T, Wang L *et al*: A program for annotating and predicting the effects of single nucleotide polymorphisms, SnpEff: SNPs in the genome of *Drosophila melanogaster* strain w1118; iso-2; iso-3. *Fly (Austin)* 2012; **6**: 80-92.
14. Ren A, Zhang D, Tian Y, Cai P, Zhang T, Hu QN: Transcriptor: a comprehensive platform for annotation of the enzymatic functions of transcripts. *Bioinformatics* 2020.
15. Richards S, Aziz N, Bale S, Bick D, Das S, Gastier-Foster J *et al*: Standards and guidelines for the interpretation of sequence variants: a joint consensus recommendation of the American College of Medical Genetics and Genomics and the Association for Molecular Pathology. *Genet Med* 2015; **17**: 405-424.
16. Castro MJ, Nunes B, de Vries B, Lemos C, Vanmolkot KR, van den Heuvel JJ *et al*: Two novel functional mutations in the Na⁺,K⁺-ATPase alpha2-subunit ATP1A2 gene in patients with familial hemiplegic migraine and associated neurological phenotypes. *Clin Genet* 2008; **73**: 37-43.
17. Pressley TA: Phylogenetic conservation of isoform-specific regions within alpha-subunit of Na⁽⁺⁾-K⁽⁺⁾-ATPase. *Am J Physiol* 1992; **262**: C743-751.
18. Jiang Y, Han Y, Petrovski S, Owzar K, Goldstein DB, Allen AS: Incorporating Functional Information in Tests of Excess De Novo Mutational Load. *Am J Hum Genet* 2015; **97**: 272-283.
19. Moya-Mendez ME, Mueller DM, Pratt M, Bonner M, Elliott C, Hunanyan A *et al*: Early onset severe ATP1A2 epileptic encephalopathy: Clinical characteristics and underlying mutations. *Epilepsy Behav* 2021; **116**: 107732.
20. Bassi MT, Bresolin N, Tonelli A, Nazos K, Crippa F, Baschiroto C *et al*: A novel mutation in the ATP1A2 gene causes alternating hemiplegia of childhood. *J Med Genet* 2004; **41**: 621-628.
21. Panagiotakaki E, Papadopoulou MT, Lesca G, Arzimanoglou A, Mikati MA: De novo mutations in CLDN5: alternating hemiplegia of childhood or not? *Brain* 2023.
22. De Fusco M, Marconi R, Silvestri L, Atorino L, Rampoldi L, Morgante L *et al*: Haploinsufficiency of ATP1A2 encoding the Na⁺/K⁺ pump alpha2 subunit associated with familial hemiplegic migraine type 2. *Nat Genet* 2003; **33**: 192-196.

23. Pietrobon D: Familial hemiplegic migraine. *Neurotherapeutics* 2007; **4**: 274-284.
24. de Vries B, Stam AH, Beker F, van den Maagdenberg AM, Vanmolkot KR, Laan L *et al*: CACNA1A mutation linking hemiplegic migraine and alternating hemiplegia of childhood. *Cephalalgia* 2008; **28**: 887-891.
25. Mikati MA, Panagiotakaki E, Arzimanoglou A: Revision of the diagnostic criteria of alternating hemiplegia of childhood. *Eur J Paediatr Neurol* 2021; **32**: A4-A5.
26. Ogiwara I, Ito K, Sawaishi Y, Osaka H, Mazaki E, Inoue I *et al*: De novo mutations of voltage-gated sodium channel alphaII gene SCN2A in intractable epilepsies. *Neurology* 2009; **73**: 1046-1053.
27. Wolff M, Johannesen KM, Hedrich UBS, Masnada S, Rubboli G, Gardella E *et al*: Genetic and phenotypic heterogeneity suggest therapeutic implications in SCN2A-related disorders. *Brain* 2017; **140**: 1316-1336.
28. Mikati MA, Maguire H, Barlow CF, Ozelius L, Breakefield XO, Klauck SM *et al*: A syndrome of autosomal dominant alternating hemiplegia: clinical presentation mimicking intractable epilepsy; chromosomal studies; and physiologic investigations. *Neurology* 1992; **42**: 2251-2257.
29. Rosewich H, Ohlenbusch A, Huppke P, Schlotawa L, Baethmann M, Carrilho I *et al*: The expanding clinical and genetic spectrum of ATP1A3-related disorders. *Neurology* 2014; **82**: 945-955.
30. Rui H, Artigas P, Roux B: The selectivity of the Na⁽⁺⁾/K⁽⁺⁾-pump is controlled by binding site protonation and self-correcting occlusion. *Elife* 2016; **5**.

Tables

Table 1 Study cohort

family ID	subject ID	phenotype	gender	trio	affected family members	genomic analysis	% of full <i>ATPIA3</i> gene^a	% of protein-coding regions of <i>ATPIA3</i>^b
ahcbh	ahcdukeepi4538bh1	atypical	female	yes	no	exome/targeted sequencing	97.44	97.8
ahcbv	ahcdukeepi4542bv1	atypical	female	no, proband only	no	exome/targeted sequencing	99.82	98.7
ahcaw	ahcdukeepi2937aw1	atypical	female	yes	no	exome/targeted sequencing	98	96.1
ahcn	ahcdukeepi3911n4	atypical	female	yes	yes, affected half-sibling (same mother)	exome/targeted sequencing	95.54	98.7
ahcbj	ahcdukeepi4512bj1	atypical	female	yes	no	exome/targeted sequencing	91.33	98.2

family ID	subject ID	phenotype	gender	trio	affected family members	genomic analysis	% of full <i>ATPIA3</i> gene^a	% of protein-coding regions of <i>ATPIA3</i>^b
ahcbw	ahcdukeepi4542bw1	atypical	male	no, proband only	no	exome/targeted sequencing	99.41	98.7
ahcao	ahcdukeepi3905ao1	atypical	male	yes	no	exome/targeted sequencing	94.83	96.6
ahcbz	ahc14A84bz1	typical	female	yes	no	exome/targeted sequencing	98.96	98.6
ahcbi	ahcdukeepi4529bi1	typical	female	yes	no	exome/targeted sequencing	97.85	98.7
ahcbd	ahcdukeepi4588bd1	typical	female	yes	no	exome/targeted sequencing	97.66	98.7
ahcx	ahcdukeepi3902x1	typical	female	no, proband only	no	exome/targeted sequencing	96.98	98.5
ahcbb	ahcdukeepi3937bb1	typical	female	no, proband only	no	exome/targeted sequencing	97.84	98.3

family ID	subject ID	phenotype	gender	trio	affected family members	genomic analysis	% of full <i>ATPIA3</i> gene ^a	% of protein-coding regions of <i>ATPIA3</i> ^b
ahcbs	ahcdukeepi4542bs1	typical	female	no, proband only	no	exome/targeted sequencing	99.99	98.7
ahcaa	ahc13A3478aa1ex	typical	female	yes	no	exome/targeted sequencing	99.74	98.7
ahcby	ahc150010by1	typical	female	yes	no	exome/targeted sequencing	99.04	98.2
dukeepi454 7	ahcdukeepi4547bf4	typical	male	yes	three additional affected full sblings	exome/targeted sequencing	97.22	98.7
ahcbo	ahcdukeepi4524bo1	typical	male	yes	no	exome/targeted sequencing	97.68	97.9
ahcbc	ahcdukeepi4593bc1	typical	male	yes	no	exome/targeted sequencing	97.08	98.7

family ID	subject ID	phenotype	gender	trio	affected family members	genomic analysis	% of full <i>ATPIA3</i> gene ^a	% of protein-coding regions of <i>ATPIA3</i> ^b
ahcad	ahc13A1635ad1ex	typical	male	yes	no	exome/targeted sequencing	99.5	98.7
ahcab	ahc13A2107ab1ex	typical	male	yes	no	exome/targeted sequencing	99.03	98.2
ahcag	ahc13A581ag1ex	typical	male	yes	no	exome/targeted sequencing	98.77	98.7
ahcah	ahc157184ah1ex	typical	male	no, proband only	no	exome/targeted sequencing	99.29	98.7
ahcbe	ahcdukeepi4580be1	atypical	female	yes	one additional affected full sibling	exome	NA	98.7
ahcav	ahcit01ap1	typical	female	yes	no	exome	NA	98.7
ahci	ahc149666i1	typical	female	yes	no	exome	NA	98.7
ahck	ahcahc2k1	typical	female	yes	no	exome	NA	98.7

family ID	subject ID	phenotype	gender	trio	affected family members	genomic analysis	% of full <i>ATPIA3</i> gene ^a	% of protein-coding regions of <i>ATPIA3</i> ^b
ahcacc	ahc13A2344ac1	typical	male	no, proband only	no	targeted sequencing of <i>SCN2A</i>	NA	NA
IT06c	IT06	typical	female	no, proband only	no	exome	NA	NA

^a Sequenced at least 10-fold in proband; ^b Sequenced at least 10-fold in proband (exome and targeted sequencing); ^c cases identified after original sequencing study. NA = not applicable.

Table 2 Candidate genetic diagnoses in *ATPIA3*-negative AHC cohort

Sample ID	inheritance	Variant ID (chr-position-ref-alt, hg19)	Variant Type	GeneName	Transcript	HGVS_c	HGVS_p	ACMG classification
ahc149666i1	<i>de novo</i>	10-62023779-C-T	snv	<i>ANK3</i>	ENST00000280772	c.514-1G>A	NA	likely pathogenic
ahc14A84bz1	<i>de novo</i>	1-160097587-G-C	snv	<i>ATPIA2</i>	ENST00000361216	c.994G>C	p.E332Q	likely pathogenic
ahcdukeepi4542bw1 ^a	inheritance unknown	1-160105782-T-A	snv	<i>ATPIA2</i>	ENST00000361216	c.2438T>A	p.M813K	likely pathogenic
ahcdukeepi4524bo1 ^a	inherited from father with hemiplegic migraine	1-160097615-G-A	snv	<i>ATPIA2</i>	ENST00000361216	c.1017+5G>A	NA	likely pathogenic
ahcdukeepi4580be1	<i>de novo</i>	15-93540315-GAA-G	indel	<i>CHD2</i>	ENST00000394196	c.3722_3723delA A	p.E1241fs	likely pathogenic

Sample ID	inheritance	Variant ID (chr-position-ref-alt, hg19)	Variant Type	GeneName	Transcript	HGVS_c	HGVS_p	ACMG classification
ahc13A581ag1ex	<i>de novo</i>	8-22864414-C-T	snv	<i>RHOBTB2</i>	ENST000002 51822	c.656C>T	p.S219F	likely pathogenic
ahcahc2k1	<i>de novo</i>	8-22861984-G-A	snv	<i>RHOBTB2</i>	ENST000002 51822	c.37G>A	p.E13K	likely pathogenic
ahcdukeepi4538bh1	<i>de novo</i>	8-22865140-G-A	snv	<i>RHOBTB2</i>	ENST000002 51822	c.1382G>A	p.R461H	pathogenic
ahcdukeepi4542bv1	inherited from unaffected father ^c	8-22862900-C-T	snv	<i>RHOBTB2</i>	ENST000002 51822	c.208C>T	p.R70*	VOUS
ahcdukeepi4593bc1	<i>de novo</i>	2-166237628-CAGA- C	indel	<i>SCN2A</i>	ENST000002 83256	c.4477_4479delG AA	p.E1493del	pathogenic
IT06 ^b	<i>de novo</i>	2-166245267-T-G	snv	<i>SCN2A</i>	ENST000002 83256	c.4951T>G	p.F1651V	likely pathogenic

Sample ID	inheritance	Variant ID (chr-position-ref-alt, hg19)	Variant Type	GeneName	Transcript	HGVS_c	HGVS_p	ACMG classification
ahc13A2344ac1 ^b	unknown	2-166243356-A-G	snv	SCN2A	ENST00000283256	c.4652A>G	p.E1551G	likely pathogenic

^aPatient previously reported in Moya-Mendez et al (2021) [19]; ^bVariants identified in separate studies (see Materials and Methods); ^cinherited determined from clinical sequencing; *VOUS* variant of unknown significant. Indel = insertion -deletion; snv = single nucleotide variation; NA = non applicable

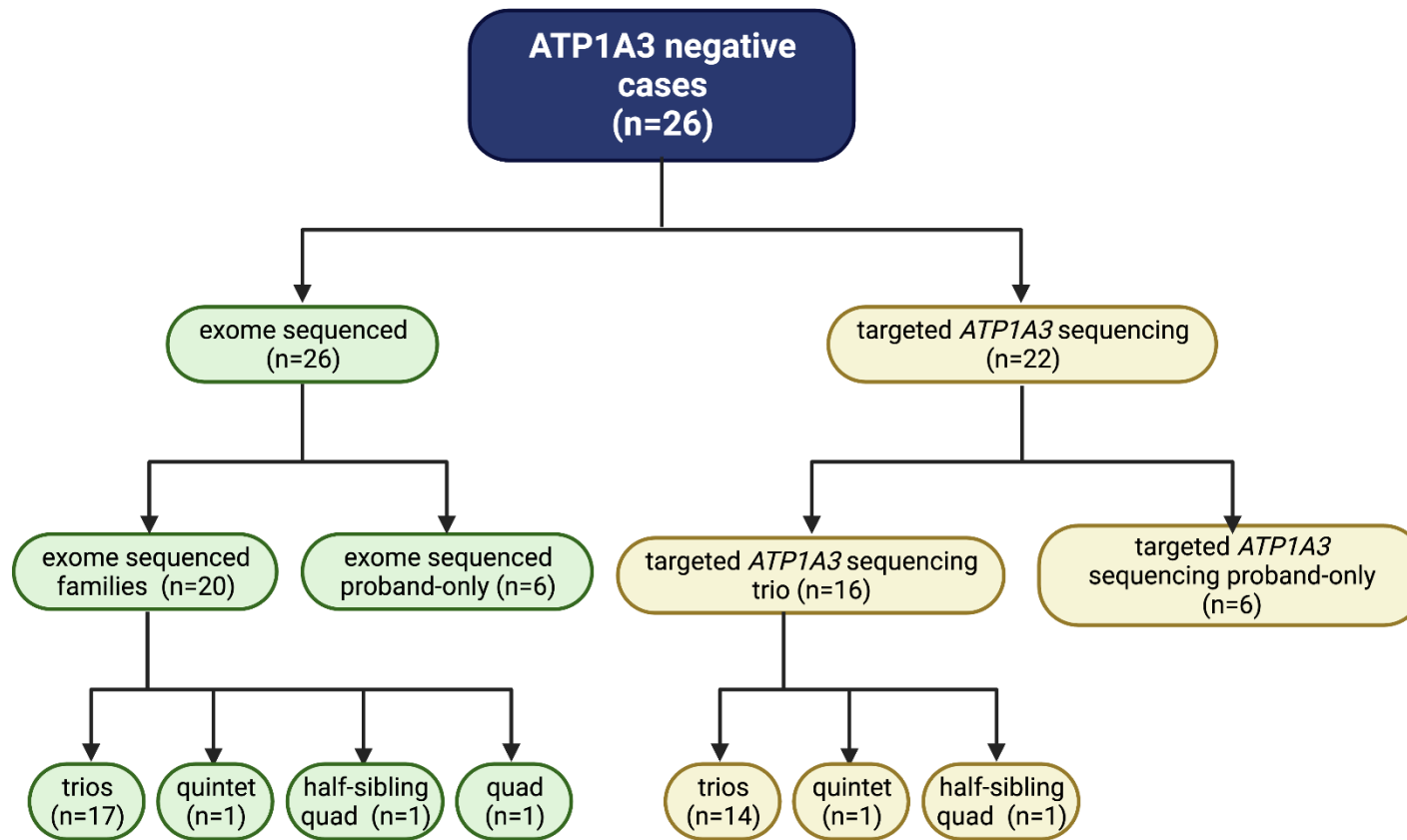


Figure 1

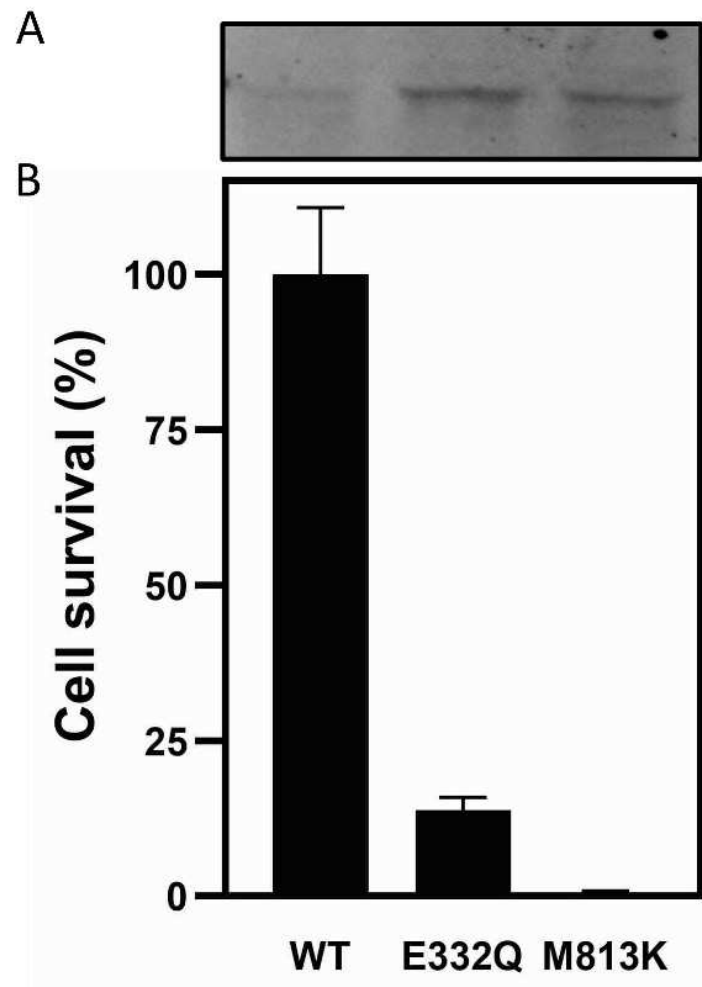


Figure 2

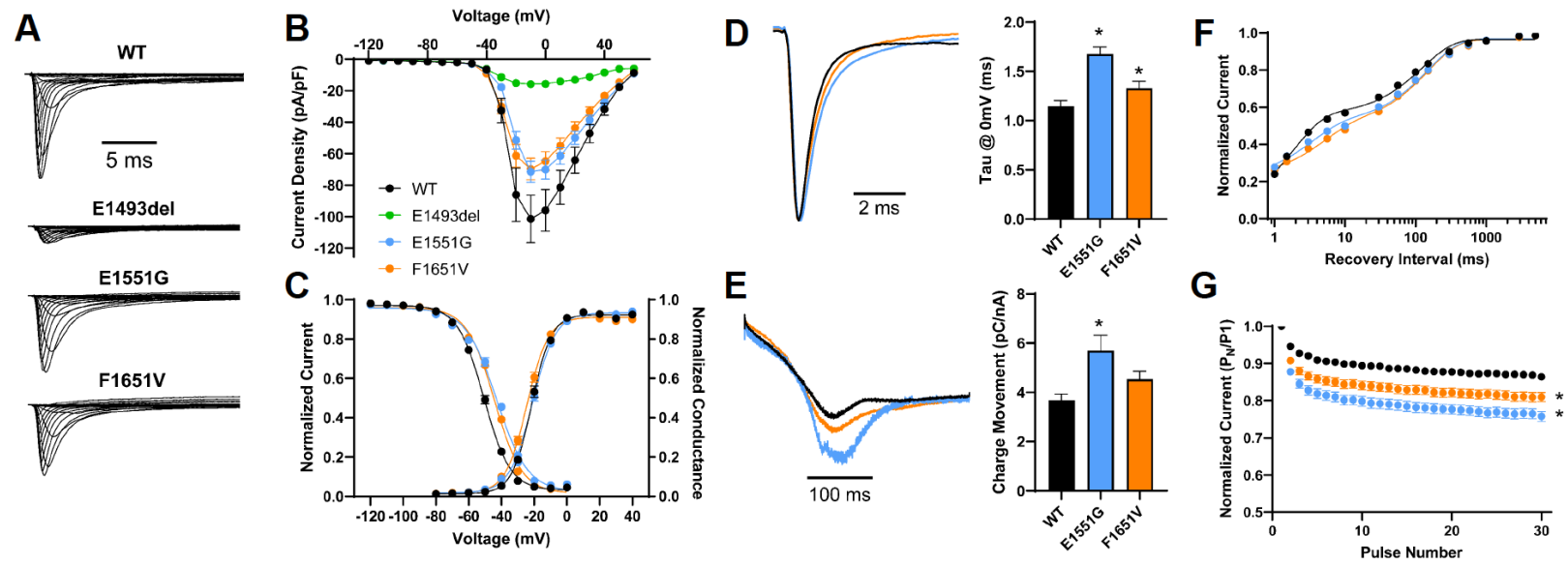


Figure 3

Supplementary Information_Consortia List

I.B.AHC Consortium

Maria Teresa Bassi¹, Claudio Zucca¹, Elisa De Grandis², Michela Stagnaro², Edvige Veneselli², Filippo Franchini³, Melania Giannotta⁴, Giuseppe Gobbi⁴, Tiziana Granata⁵, Nardo Nardocci⁵, Francesca Ragona⁵, Fiorella Gurrieri⁶, Giovanni Neri⁶, Francesco Danilo Tiziano⁶, Emanuela Abiussi⁷, Alessandro Capuano⁸, Federico Vigeveno⁸, Rosaria Vavassori⁹

¹ *Scientific Institute IRCCS E. Medea, Bosisio Parini (LC), Italy*

² *Istituto G. Gaslini, University of Genoa, Genoa, Italy*

³ *A.I.S.EA Onlus, Milan, Italy*

⁴ *IRCCS Istituto delle Scienze Neurologiche di Bologna, Bologna, Italy*

⁵ *IRCCS Foundation Neurological Institute C. Besta, Milan, Italy*

⁶ *Istituto di Medicina Genomica Università Cattolica del S. Cuore, Rome, Italy*

⁷ *Università Cattolica del Sacro Cuore, Roma, Italy*

⁸ *Bambino Gesù Children's Hospital, IRCCS, Rome, Italy*

⁹ *Euro-Mediterranean Institute for Science and Technology I.E.ME.S.T.,Palermo, Italy*

IAHCRC Consortium

Mohamad A Mikati¹, Andrew P Landstrom^{2,3}, Mary E Moya-Mendez^{2,3}, Erin L Heinzen^{4,5}, Eleni Panagiotakaki⁶, Alexis Arzimanoglou^{6,7}, Gaetan Lesca⁸, Stéphane Auvin⁹, Domitille Gras⁹, Odile Boespflug-Tanguy⁹, Diane Doummar¹⁰, Marie-Laure Moutard¹⁰, Thierry Billette de Villemeur¹⁰, Emmanuel Flamand-Roze¹¹, Isabelle An¹¹, Fanny Mochel¹¹, Rima Nabbout¹², Nadia Bahi-Buisson¹², François Rivier¹³, Agathe Roubertie¹³, Arn MJM van den Maagdenberg¹⁴, Cacha Peeters-Scholte¹⁴, Helen Cross¹⁵, Katharina Vezyroglou¹⁵, Sanjay Sisodiya¹⁶, Simona Balestrini¹⁶, Juan Kaski¹⁶, Giovanni Neri¹⁷, Fiorella Gurrieri¹⁷, Danilo Tiziano¹⁷, Edvige Veneselli¹⁸, Elisa De Grandis¹⁸, Michela Stagnaro¹⁸, Giuseppe Gobbi¹⁹, Melania Giannotta¹⁹, Mariateresa Bassi²⁰, Claudio Zucca²¹, Federico Vigeveno²², Alessandro Capuano²², Massimiliano Valeriani²², Tiziana Granata²³, Nardo Nardocci²³, Francesca Ragona²³, Renzo Guerrini²⁴, Bartolomeo Sammartino²⁵, Francesco Cappello²⁵, Giosuè lo Bosco²⁵, Rosaria Vavassori²⁵, Andrey Megvinov²⁵, Jaume Campistol²⁶, Carmen Fons²⁶, Jennifer Anticono²⁶, Sarah Weckhuysen²⁷, Sona Nevsimalova²⁸, David Kemlink²⁸, Anna Krepelova²⁹, Pavol Sykora³⁰, Miriam Kolnikova³⁰, Ingrid Sheffer³¹, Steven Petrou³², Dimitrios Zafeiriou³³, Sotiria Mastrogianni³⁴, Roser Pons³⁵, Vesna Brankovic³⁶, Nebojsa Jovic³⁶, Vedrana Milic Rasic³⁶, Ana Potic³⁶, Yi Wang³⁷, Bingbing Wu³⁸, Maria Mazurkiewicz-Beldzińska³⁹, Agniescka Sawicka³⁹, Marta Zawadzka³⁹, Maria Szmuda³⁹, Sergiu Groppa⁴⁰, Holger Kuntze⁴⁰, Christian Dresel⁴⁰, Tajul Tajudin⁴¹, Marina Gáinza-Lein⁴², Mònica Troncoso⁴², Mario Matamala⁴²

-
- ¹ *Division of Pediatric Neurology and Developmental Medicine, Duke University, Durham, NC, USA*
 - ² *Department of Pediatrics, Duke University, Durham, NC, USA*
 - ³ *Division of Pediatric Cardiology, Duke University, Durham, NC, USA*
 - ⁴ *Division of Pharmacology and Experimental Therapeutics, Eshelman School of Pharmacy, University of North Carolina at Chapel Hill, Chapel Hill, NC, USA*
 - ⁵ *Department of Genetics, School of Medicine, University of North Carolina at Chapel Hill, Chapel Hill, NC, USA*
 - ⁶ *Department of Paediatric Clinical Epileptology, Sleep Disorders and Functional Neurology, Member of the ERN EpiCare, University Hospitals of Lyon (HCL), Lyon, France*
 - ⁷ *Department of Child Neurology and Epilepsy Research Unit, Member of the ERN EpiCARE, Hospital San Juan de Dios, Barcelona, Spain*
 - ⁸ *Department of Medical Genetics, University Hospital of Lyon and Claude Bernard Lyon I University, Lyon France - Pathophysiology and Genetics of Neuron and Muscle (PNMG), UCBL, CNRS UMR5261 - INSERM UI315, Lyon, France*
 - ⁹ *Child Neurology Department, University Hospital Robert Debré (AP-HP), Inserm U1141, Paris, France*
 - ¹⁰ *Service de Neuropédiatrie, University Hospital Trousseau (AP-HP); Centre Neurogénétique Mouvements Anormaux de l'enfant à l'adulte, Paris, France*
 - ¹¹ *Département des Maladies du Système Nerveux, University Hospital Salpêtrière (AP-HP), Paris, France*
 - ¹² *Department of Pediatric Neurology, University Hospital Necker-Enfants Malades (AP-HP), Paris, France*
 - ¹³ *Child Neurology Department, University Hospital of Montpellier, Hôpital Gui de Chauliac, Montpellier, France*
 - ¹⁴ *Departments of Human Genetics and Neurology, Leiden University Medical Centre, Leiden, The Netherlands*
 - ¹⁵ *Institute of Child Health, University College London, London, UK*
 - ¹⁶ *Institute of Neurology, University College London, London, UK*
 - ¹⁷ *Institute of Medical Genetics, Università Cattolica S. Cuore School of Medicine, Rome, Italy*
 - ¹⁸ *Department of Child Neuropsychiatry, G. Gaslini Scientific Institute and Hospital, University of Genoa, Genoa, Italy*
 - ¹⁹ *Child Neurology Unit, Institute of Neuroscience and Bellaria Hospital, Bologna, Italy*
 - ²⁰ *Laboratory of Molecular Biology, Scientific Institute IRCCS Eugenio Medea, Bosisio Parini (LC), Italy*
 - ²¹ *Clinical Neurophysiology Unit, Scientific Institute IRCCS Eugenio Medea, Bosisio Parini (LC), Italy*
 - ²² *Division of Neurology, Bambino Gesù Children's Hospital, Rome, Italy*
 - ²³ *Department of Child Neurology, National Neurological Institute C. Besta, Milan, Italy*
 - ²⁴ *Department of Neuroscience, Children's Hospital A. Meyer, University of Florence, Florence, Italy*
 - ²⁵ *Euro-Mediterranean Institute of Science and Technology, Palermo, Italy*
 - ²⁶ *Department of Child Neurology, Hospital Sant Joan de Déu, Barcelona University, Barcelona, Spain*
 - ²⁷ *VIB CMN (Center for Molecular Neurology), Applied and Translational Neurogenomics Group, University of Antwerp – CDE, Antwerp, Belgium*
 - ²⁸ *Department of Neurology and Center of Clinical Neurosciences, Charles University, 1st Faculty of Medicine and General Teaching Hospital, Prague, Czech Republic*
 - ²⁹ *Institute of Biology and Medical Genetics, Charles University, 2nd Faculty of Medicine and Motol Teaching Hospital, Prague, Czech Republic*
 - ³⁰ *Department of Pediatric Neurology, Komenius University, Faculty of Medicine and Pediatric Teaching Hospital, Bratislava, Slovakia*
 - ³¹ *Department of Paediatrics and Department of Medicine, University of Melbourne, Austin Health, Melbourne, Australia*
 - ³² *Ion Channels & Disease Group, Epilepsy Division, The Florey Institute of Neuroscience and Mental Health, Parkville, Victoria, Australia*
 - ³³ *1st Department of Paediatrics, Aristotle University of Thessaloniki, "Hippokratio" General Hospital, Thessaloniki, Greece*

- ³⁴ *Department of Neurology, Children's Hospital of Athens "P. and A. Kyriaku", Athens, Greece*
- ³⁵ *1st Department of Pediatrics, National and Kapodistrian University of Athens, Agia Sofia Hospital, Athens, Greece*
- ³⁶ *Clinic for Child Neurology and Psychiatry, Medical Faculty University of Belgrade, Belgrade, Serbia*
- ³⁷ *Department of Pediatric Neurology, Children's Hospital of Fudan University, Shanghai, China*
- ³⁸ *Molecular Diagnostic Center, Children's Hospital of Fudan University, Shanghai, China*
- ³⁹ *Department of Developmental Neurology, Clinical Centre Medical University of Gdańsk, Gdańsk, Poland*
- ⁴⁰ *Department of Movement Disorders and Neurostimulation, Neurology Institute University of Mainz, Mainz, Germany*
- ⁴¹ *Department of Pediatrics, Hospital Sultan Ismail, Johor Bahru, Johor Bahru, Malaysia*
- ⁴² *Department of Pediatric Neurology, Hospital Clínico San Borja Arriarán - Universidad de Chile, Santiago, Chile*

Supplementary Table 1. Clinical phenotypes of study participants.

Family identifier	ahcaw	ahcx	ahcao	ahcn	ahcn
Sample identifier	ahcdukeepi2937aw1	ahcdukeepi3902x1	ahcdukeepi3905ao1	ahcdukeepi3911n4	ahcdukeepi3144n1
onset of symptoms before 18 months (yes/no)	yes	yes	no	yes	yes
repeated episodes of hemiplegia that sometimes involve both sides of the body (yes/no)	yes	yes	no	yes	yes
quadriplegia that occurs as an isolated incident or as part of a hemiplegic attack (yes/no)	no	yes	yes	yes	yes
relief from symptoms upon sleeping (yes/no)	no	yes	no	no	yes
paroxysmal attacks such as dystonia, tonic episodes, abnormal eye movements or autonomic dysfunction (yes/no)	unknown	yes	yes	yes	yes

evidence of developmental delay or neurological abnormalities such as choreoathetosis, ataxia or cognitive disability (yes/no)	yes	yes	no	yes	yes
idiopathic (cannot be attributed to another cause) (yes/no)	yes	yes	yes	yes	yes
Migraine diagnosis (yes/no)	no	yes	no	no	no
hemiplegic migraine diagnosis (yes/no)	no	no	no	no	no
affected siblings?	no	no	no	yes	yes
Phenotype summarized	atypical	typical	atypical	atypical	typical

ahcbb	ahcbj	ahcbo	ahcbi	ahcbh	ahcbf
ahcdukeepi3937bb1	ahcdukeepi4512bj1	ahcdukeepi4524bo1	ahcdukeepi4529bi1	ahcdukeepi4538bh1	ahcdukeepi4547bf4
no	yes	yes	yes	yes	yes
yes	yes	yes	yes	no	yes
yes	yes	yes	yes	no	yes
yes	yes	yes	yes	yes	yes
yes	yes	yes	yes	yes	yes

yes	no	yes	yes	yes	yes
yes	yes	yes	yes	yes	yes
no	no	no	no	no	no
no	no	no	no	no	no
no	no	no	no	no	yes
typical	atypical	typical	typical	atypical	typical

ahcbf	ahcbf	ahcbe	ahcbe	ahcbd	ahcbc
ahcdukeepi4550bf5	ahcdukeepi4551bf1	ahcdukeepi4580be1	ahcdukeepi4583be4	ahcdukeepi4588bd1	ahcdukeepi4593bc1
yes	yes	no	no	yes	yes
yes	yes	yes	no	yes	yes
yes	yes	no	unknown	yes	yes
yes	unknown	no	no	unknown	yes
yes	yes	no	no	yes	yes

yes	yes	yes	no	yes	yes
yes	yes	yes	yes	yes	yes
no	no	yes	yes	no	no
no	no	yes	no	no	no
yes	yes	yes	yes	no	
typical	typical	atypical	atypical	typical	typical

ahcbs	ahcbw	ahcbv	NA	ahcad	ahcbz
ahcdukeepi4542bs1	ahcdukeepi4542bw1	ahcdukeepi4542bv1	ahcit01ap1	NA	ahc13A1635ad1ex
yes	yes	yes	yes	yes	yes
yes	yes	yes	yes	yes	yes
yes	no	unknown	yes	yes	yes
yes	no	unknown	yes	yes	yes
yes	no	yes	yes	yes	yes

yes	yes	yes	yes	yes	yes
yes	yes	yes	yes	yes	yes
no	no	no	No	No	No
no	no	no	No	No	No
no	no	no			
typical	atypical	atypical	typical	typical	typical

ahct	ahcaa	ahcag	ahci	ahcby	ahcah
ahc14A84bz1	ahc13A2107ab1ex	ahc13A3478aa1ex	ahc13A581ag1ex	ahc149666i1	ahc150010by1
yes	yes	yes	yes	yes	yes
yes	yes	yes	yes	yes	yes
yes	yes	yes	yes	yes	yes
yes	yes	yes	yes	yes	yes
yes	yes	yes	yes	yes	yes

yes	yes	yes	yes	yes	yes
yes	yes	yes	yes	yes	yes
no	no	no	no	no	no
No	no	no	no	no	no
typical	typical	typical	typical	typical	typical

ahck	NA	NA
ahc157184ah1ex	ahcahc2k1	ahc13A2344ac1
yes	yes	yes
yes	yes	yes
yes	yes	yes
yes	yes	yes
yes	yes	yes

yes	yes	yes
yes	yes	yes
no	no	no
no	no	no
typical	typical	typical

Supplementary Table 3: Functional Properties of AHC2-associated SCN2A Variants

	WT	p.E1493del	p.E1551G	p.F1651V
Current Amplitude (pA/pF)	Mean±SEM(SD)	Mean±SEM(SD)	Mean±SEM(SD)	Mean±SEM(SD)
<i>Raw Value</i>	-96.0 ±13.2(97.9)	-15.7±1.2(6.1)	-70.0±6.2(53.6)	-64.7±6.1(54.9)
<i>% WT</i>	100.0±13.7(101.8)	16.2±1.2(6.5)	73.4±6.6(56.5)	67.7±6.4(57.5)
<i>n</i>	55	28	74	81
<i>p-value</i>		<0.0001	0.6967	0.1026
V_{1/2} Activation (mV)				
<i>Raw Value</i>	-20.9±0.8(5.9)	ND	-21.1±0.7(6.3)	-23.7±0.8(7.0)
<i>Δ WT</i>	0.0±0.8(5.8)	ND	-0.3±0.7(6.3)	-2.8±0.8(7.0)
<i>n</i>	55	0	74	81
<i>p-value</i>		ND	0.3158	0.7884
V_{1/2} Inactivation (mV)				
<i>Raw Value</i>	-51.0±0.7(7.9)	ND	-44.6±1.0(9.6)	-45.4±0.7(7.5)
<i>Δ WT</i>	0.0±0.7(7.5)	ND	6.3±1.0(9.5)	5.5±0.7(7.5)
<i>n</i>	128	0	89	118
<i>p-value</i>		ND	<0.0001	<0.0001
Recovery Tau Fast (ms)				
<i>Raw Value</i>	3.1±1.1(9.3)	ND	12.5±3.6(27.3)	6.7±1.0(8.6)
<i>Fold WT</i>	1.0±0.3(2.5)	ND	4.7±1.6(12.1)	2.1±(0.3(2.5)
<i>n</i>	75	0	57	74
<i>p-value</i>		ND	<0.0001	<0.0001
Recovery Tau Slow (ms)				
<i>Raw Value</i>	146.9±10.4(137.8)	ND	196.4±17.7(135.1)	158.5±9.6(81.9)
<i>Fold WT</i>	1.0±0.1(0.9)	ND	1.3±0.1(1.0)	1.1±0.1(0.6)
<i>n</i>	75	0	57	74
<i>p-value</i>		ND	0.0018	0.1101
Recovery % Fast				
<i>Raw Value</i>	59.2±1.4(12.1)	ND	47.5±1.8(13.6)	41.4±1.5(12.7)
<i>% WT</i>	100.0±2.3(20.0)	ND	80.7±2.9(22.2)	70.5±2.4(20.8)
<i>n</i>	75	0	57	74
<i>p-value</i>		ND	<0.0001	<0.0001
Use-Dependent Rundown (P₃₀/P₁)				
<i>Raw Value</i>	86.4±0.9(9.8)	ND	75.8±1.4(12.8)	81.0±1.2(13.1)
<i>% WT</i>	100.0±1.0(11.2)	ND	88.3±1.6(15.0)	94.2±1.4(15.1)
<i>n</i>	120	0	89	115
<i>p-value</i>		ND	<0.0001	0.0027
Inactivation Tau (ms)				
<i>Raw Value</i>	1.1±0.1(0.7)	ND	1.7±0.1(0.7)	1.3±0.1(0.8)
<i>% WT</i>	100.0±5.0(57.4)	ND	152.3±6.5(65.2)	116.0±5.5(63.7)
<i>n</i>	134	0	102	136
<i>p-value</i>		ND	<0.0001	0.0028
Ramp Current (pC/nA)				
<i>Raw Value</i>	3.7±0.2(1.6)	ND	5.7±0.6(2.2)	4.5±0.3(2.2)
<i>% WT</i>	100.0±6.6(42.6)	ND	140.8±16.5(57.2)	112.5±7.7(50.8)
<i>n</i>	42	0	12	44
<i>p-value</i>		ND	0.0073	0.0936
Persistent Current (% Peak)				
<i>Raw Value</i>	2.1±0.1(1.0)	ND	2.2±0.3(1.2)	2.4±0.2(1.1)
<i>% WT</i>	100.0±7.0(44.6)	ND	95.4±13.6(47.1)	102.3±6.6(42.6)
<i>n</i>	41	0	12	41
<i>p-value</i>		ND	>0.9999	0.5488

Supplementary Table 2. Rare variants and genotypes identified in exome sequenced *ATP1A3* negative AHC cohort

ACMG genetic diagnosis	Sample ID	Phenotype summarized	SeqType	inheritance
VOUS, splicing region variant inherited from father	ahcdukeepi4524bo1	typical	exome	rare heterozygous variant, inherited from
VOUS, inherited from healthy mom per clinical testing	ahcdukeepi4542bv1	atypical	exome	rare heterozygous variant, inheritance u
pathogenic	ahcdukeepi4538bh1	atypical	exome	de novo
pathogenic	ahcdukeepi4593bc1	typical	exome	de novo
likely pathogenic	ahc14A84bz1	typical	exome	de novo
likely pathogenic	ahcdukeepi4542bw1	atypical	exome	rare heterozygous variant, inheritance u
likely pathogenic	ahcdukeepi4580be1	atypical	exome	de novo
likely pathogenic	ahc13A581ag1ex	typical	exome	de novo
likely pathogenic	ahc149666i1	typical	exome	de novo
likely pathogenic	ahcahc2k1	typical	exome	de novo
	ahcit01ap1	typical	exome	compound heterozygote
	ahcit01ap1	typical	exome	rare heterozygous variant, inherited from
	ahcit01ap1	typical	exome	rare heterozygous variant, inherited from
	ahcit01ap1	typical	exome	rare heterozygous variant, inherited from
	ahcit01ap1	typical	exome	rare heterozygous variant, inherited from
	ahcit01ap1	typical	exome	rare heterozygous variant, inherited from
	ahcit01ap1	typical	exome	rare heterozygous variant, inherited from
	ahcit01ap1	typical	exome	rare heterozygous variant, inheritance u
	ahcit01ap1	typical	exome	rare heterozygous variant, inherited from
	ahcit01ap1	typical	exome	compound heterozygote
	ahcit01ap1	typical	exome	rare heterozygous variant, inherited from
	ahcit01ap1	typical	exome	rare heterozygous variant, inherited from
	ahcit01ap1	typical	exome	rare heterozygous variant, inherited from
	ahcit01ap1	typical	exome	rare heterozygous variant, inherited from
	ahcit01ap1	typical	exome	de novo
	ahcit01ap1	typical	exome	rare heterozygous variant, inherited from
	ahcit01ap1	typical	exome	rare heterozygous variant, inherited from
	ahcit01ap1	typical	exome	rare heterozygous variant, inherited from
	ahcit01ap1	typical	exome	rare heterozygous variant, inherited from
	ahcit01ap1	typical	exome	rare heterozygous variant, inherited from

Variant ID (chr-position-ref-alt)	Variant Type	GeneName	Effect	Transcript	HGVS_c	HGVS_p	Varkant allele	Polyphen2 (hu)
1-160097615-G-A	snv	ATP1A2	splice_region	ENST0000036	c.1017+5G>A	NA	0,4444	-
8-22862900-C-T	snv	RHOBTB2	stop_gained	ENST0000025	c.208C>T	p.Arg70*	0,4667	-
8-22865140-G-A	snv	RHOBTB2	missense_vari	ENST0000025	c.1382G>A	p.Arg461His	0,4783	1
2-166237628-CAGA-C	indel	SCN2A	conservative_i	ENST0000028	c.4477_4479d	p.Glu1493del	0,4097	-
1-160097587-G-C	snv	ATP1A2	missense_vari	ENST0000036	c.994G>C	p.Glu332Gln	0,48	1
1-160105782-T-A	snv	ATP1A2	missense_vari	ENST0000036	c.2438T>A	p.Met813Lys	0,4839	0,998
15-93540315-GAA-G	indel	CHD2	frameshift_var	ENST0000039	c.3722_3723d	p.Glu1241fs	0,5	-
8-22864414-C-T	snv	RHOBTB2	missense_vari	ENST0000025	c.656C>T	p.Ser219Phe	0,6226	0,995
10-62023779-C-T	snv	ANK3	splice_acceptc	ENST0000028	c.514-1G>A		0,4778	-
8-22861984-G-A	snv	RHOBTB2	missense_vari	ENST0000025	c.37G>A	p.Glu13Lys	0,4464	0,999
14-105408953-G-A, 14-1054132	snv, snv	AHNAK2	missense_vari	ENST0000033	c.12835C>T, c.	p.Arg4279Trp,	0,5541, 0,5895	0,995, 0,897
19-49965935-G-A	snv	ALDH16A1	missense_vari	ENST0000029	c.1021G>A	p.Asp341Asn	0,5625	1
19-36050897-T-A	snv	ATP4A	missense_vari	ENST0000026	c.866A>T	p.Glu289Val	0,4423	0,645
3-142241679-C-A	snv	ATR	missense_vari	ENST0000035	c.4157G>T	p.Gly1386Val	0,4316	0,789
16-19562533-A-G	snv	CCP110	missense_vari	ENST0000038	c.3002A>G	p.Lys1001Arg	0,4615	0,801
3-46414906-A-C	snv	CCR5	missense_vari	ENST0000029	c.513A>C	p.Lys171Asn	0,4016	0,694
11-67848929-G-A	snv	CHKA	splice_region	ENST0000026	c.463-5C>T	NA	0,3774	-
10-71637826-G-A	snv	COL13A1	splice_region	ENST0000047	c.462+5G>A	NA	0,6087	-
2-136736557-AGC-TTT	snv	DARS	splice_region	ENST0000047	n.429_431de	NA	0,3333	-
2-71828644-A-T	snv	DYSF	missense_vari	ENST0000025	c.3859A>T	p.Ile1287Phe	0,4714	0,767
2-71780972-A-G, 2-71828644-A	snv, snv	DYSF	missense_vari	ENST0000025	c.1966A>G, c.3	p.Lys656Glu, p.	0,3977, 0,4714	0,997, 0,767
20-54941119-C-T	snv	FAM210B	splice_region	ENST0000003	c.363-8C>T	NA	0,4912	-
17-18671856-G-A	snv	FBXW10	missense_vari	ENST0000030	c.1714G>A	p.Gly572Ser	0,5281	1
1-157504544-AG-A	indel	FCRL5	frameshift_var	ENST0000035	c.1540delC	p.Leu514fs	0,3924	-
6-167446109-A-G	snv	FGFR1OP	missense_vari	ENST0000034	c.947A>G	p.Asp316Gly	0,48	0,959
17-72843517-G-C	snv	GRIN2C	missense_vari	ENST0000029	c.1931C>G	p.Thr644Arg	0,4685	0,999
14-75936104-A-G	snv	JDP2	missense_vari	ENST0000026	c.451A>G	p.Ile151Val	0,4565	0,978
6-18215250-G-T	snv	KDM1B	missense_vari	ENST0000029	c.1426G>T	p.Val476Leu	0,5172	0,928
1-245861440-T-C	snv	KIF26B	missense_vari	ENST0000036	c.4714T>C	p.Ser1572Pro	0,5	0,508
1-43212957-G-A	snv	LEPRE1	stop_gained	ENST0000023	c.2041C>T	p.Arg681*	0,5417	-
12-85445971-T-G	snv	LRRIQ1	missense_vari	ENST0000039	c.695T>G	p.Met232Arg	0,4868	0,851

2-119727818-G-A	snv	MARCO	missense_vari:ENST0000032`c.328G>A	p.Ala110Thr	0,4167	0,956
19-1360395-A-G	snv	MUM1	missense_vari:ENST0000031`c.271A>G	p.Ser91Gly	0,5577	0,44
10-115661458-TG-T	indel	NHLRC2	frameshift_var ENST0000036!c.1175delG	p.Gly392fs	0,4526	-
11-56431283-G-A	snv	OR5AR1	missense_vari:ENST0000030`c.122G>A	p.Gly41Glu	0,5225	0,999
8-107718701-GC-AT	snv	OXR1	missense_vari:ENST0000031`c.931_932delC	p.Ala311Ile	0,4537	0,832
11-73008349-C-G	snv	P2RY6	stop_gained ENST0000034!c.786C>G	p.Tyr262*	0,5294	-
13-25023959-A-C	snv	PARP4	splice_region ENST000003!c.3015-4T>G	NA	0,4643	-
5-141244307-G-A	snv	PCDH1	missense_vari:ENST0000028`c.1589C>T	p.Ala530Val	0,52	0,999
2-120362375-T-TG	indel	PCDP1	splice_region ENST000002!c.*247+7_*2`	NA	0,5211	-
6-149838551-CAT-C	indel	PPIL4	frameshift_var ENST0000025`c.1016_1017d	p.Tyr339fs	0,5455	-
20-37182615-C-G	snv	RALGAPB	missense_vari:ENST0000026`c.3268C>G	p.Pro1090Ala	0,5556	0,999
8-145741418-T-C	snv	RECQL4	missense_vari:ENST0000042!c.1085A>G	p.His362Arg	0,5833	0,953
3-49742550-C-A	snv	RNF123	missense_vari:ENST0000032`c.2093C>A	p.Pro698His	0,5192	0,838
16-836252-G-C	snv	RPUSD1	missense_vari:ENST0000000`c.637C>G	p.Leu213Val	0,4783	0,999
21-46951314-G-C	snv	SLC19A1	missense_vari:ENST0000031`c.938C>G	p.Ser313Cys	0,4828	0,997
4-20255595-A-G	snv	SLIT2	missense_vari:ENST0000027`c.157A>G	p.Ile53Val	0,4722	0,506
3-4461821-C-A	snv	SUMF1	missense_vari:ENST0000027`c.529G>T	p.Ala177Ser	0,4717	0,718
14-20876231-G-T	snv	TEP1	missense_vari:ENST0000026`c.368C>A	p.Ser123Tyr	0,4876	0,781
3-21606173-C-A	snv	ZNF385D	missense_vari:ENST0000028`c.169G>T	p.Asp57Tyr	0,4299	0,948
1-247264087-GT-TG	snv	ZNF669	missense_vari:ENST0000034`c.983_984delA	p.His328Pro	0,529	0,948
5-179078646-C-G	snv	AC136604.1	stop_gained ENST0000041!c.129C>G	p.Tyr43*	0,4737	-
18-56171349-C-G	snv	ALPK2	missense_vari:ENST0000036`c.6061G>C	p.Glu2021Gln	0,3947	0,93
15-83328418-G-A	snv	AP3B2	missense_vari:ENST0000026`c.3143C>T	p.Thr1048Ile	0,5185	0,507
22-25853373-G-A	snv	CRYBB2P1	splice_region ENST000003!n.266+5G>A	NA	0,5385	-
6-31695329-G-T	snv	DDAH2	missense_vari:ENST0000037!c.732C>A	p.Asn244Lys	0,5843	0,444
6-20490645-A-T	snv	E2F3	missense_vari:ENST0000034!c.1382A>T	p.Asp461Val	0,4433	0,462
9-140729361-G-C	snv	EHMT1	missense_vari:ENST0000046!c.3853G>C	p.Gly1285Arg	0,5714	1
5-65346629-ATTCT-A	indel	ERBB2IP	frameshift_var ENST0000028`c.1925_1928d	p.Ser642fs	0,5316	-
X-54777806-A-T	snv	ITIH6	missense_vari:ENST0000021!c.3360T>A	p.His1120Gln	1	0,904
8-36644891-G-C	snv	KCNU1	missense_vari:ENST0000039!c.263G>C	p.Arg88Pro	0,4588	0,974
12-39701436-GC-AA	snv	KIF21A	missense_vari:ENST0000036`c.4372_4373d	p.Ala1458Phe	0,4541	0,924
9-21333741-T-C	snv	KLHL9	missense_vari:ENST0000035!c.1118A>G	p.Asp373Gly	0,4651	0,996
17-30348611-T-C	snv	LRRC37B	missense_vari:ENST0000032`c.527T>C	p.Leu176Pro	0,4138	0,902

5-66460070-A-G	snv	MAST4	missense_vari:ENST0000026:c.4481A>G	p.Tyr1494Cys	0,4098	0,996
15-94858839-C-G	snv	MCTP2	missense_vari:ENST0000035:c.610C>G	p.Arg204Gly	0,5909	0,97
11-46403656-C-T	snv	MDK	missense_vari:ENST0000035:c.49C>T	p.Leu17Phe	0,4433	0,991
2-157186384-G-C	snv	NR4A2	missense_vari:ENST0000033:c.315C>G	p.His105Gln	0,5283	0,469
3-52282724-C-T	snv	PPM1M	splice_region ENST000002:c.495+8C>T	NA	0,5417	-
3-113795663-G-A	snv	QTRTD1	missense_vari:ENST0000028:c.620G>A	p.Arg207Gln	0,413	0,904
3-30029716-T-G	snv	RBMS3	splice_donor_ ENST0000027:c.1131+2T>G	NA	0,3953	-
4-179208439-A-G	snv	RP11-84H6.1	splice_region ENST000004:n.591A>G	NA	0,3889	-
3-63820815-ACTATTCTACTT-indel	indel	THOC7	splice_region ENST000002:c.547+3_547	NA	0,4038	-
12-109535487-G-A	snv	UNG	start_lost ENST0000024:c.3G>A	p.Met1?	0,3925	-
18-74637501-T-G	snv	ZNF236	missense_vari:ENST0000025:c.4012T>G	p.Ser1338Ala	0,34	0,99
16-3443754-T-C	snv	ZSCAN32	missense_vari:ENST0000039:c.427A>G	p.Thr143Ala	0,3659	0,636
3-132278755-G-T	snv	ACAD11	missense_vari:ENST0000026:c.2150C>A	p.Ala717Asp	0,6	0,614
3-132294758-C-G	snv	ACAD11	missense_vari:ENST0000026:c.1859G>C	p.Gly620Ala	0,56	1
17-7804010-C-T	snv	CHD3	missense_vari:ENST0000033:c.2939C>T	p.Thr980Ile	0,5043	0,974
17-40843941-T-C	snv	CNTNAP1	missense_vari:ENST0000026:c.2462T>C	p.Val821Ala	0,3333	0,626
X-107403794-G-A	snv	COL4A6	missense_vari:ENST0000033:c.4424C>T	p.Ser1475Leu	0,5517	0,999
3-9757718-G-A	snv	CPNE9	missense_vari:ENST0000038:c.883G>A	p.Gly295Arg	0,5556	0,767
X-47582924-A-G	snv	CXXC1P1	splice_acceptc ENST0000048:n.196-2A>G	NA	0,4375	-
5-139060817-A-G	snv	CXXC5	missense_vari:ENST0000030:c.709A>G	p.Met237Val	0,4433	0,914
2-172398139-C-A	snv	CYBRD1	missense_vari:ENST0000032:c.238C>A	p.Leu80Ile	0,5455	0,72
11-674607-T-TGGCTTGCTC	indel	DEAF1	conservative_i ENST0000033:c.1156_1164d	p.Ala388_Lys3	0,4677	-
22-24179974-C-T	snv	DERL3	stop_gained ENST0000031:c.395G>A	p.Trp132*	0,5	-
14-21215905-GA-G	indel	EDDM3A	frameshift_var ENST0000032:c.171delA	p.Glu58fs	0,5258	-
17-18907171-G-T	snv	FAM83G	missense_vari:ENST0000034:c.184C>A	p.Leu62Met	0,4409	0,997
2-25387698-G-A	snv	POMC	splice_region ENST000002:c.-50-7C>T	NA	0,5319	-
13-114784383-C-A	snv	RASA3	missense_vari:ENST0000033:c.798G>T	p.Gln266His	0,4821	0,789
10-99150266-T-C	snv	RRP12	missense_vari:ENST0000037:c.667A>G	p.Lys223Glu	0,4857	0,598
19-39408365-G-C	snv	SARS2	missense_vari:ENST0000022:c.1159C>G	p.Arg387Gly	0,6667	0,987
14-81954251-A-AG	indel	SEL1L	frameshift_var ENST0000033:c.1430dupC	p.Ala478fs	0,4526	-
17-26905766-T-G	snv	SPAG5	missense_vari:ENST0000032:c.3122A>C	p.Glu1041Ala	0,5854	0,999
13-46287943-GG-CT	snv	SPERT	stop_gained ENST0000031:c.783_784delC	p.LeuGlu261*	0,4	-
22-42271557-G-GCTCT	indel	SREBF2	frameshift_var ENST0000036:c.1215_1216ir	p.Gly406fs	0,4615	-

22-42271559-GCA-G	indel	SREBF2	frameshift_var	ENST0000036:c.1218_1219d	p.Ile407fs	0,4615	-
22-42271562-TCGACCTA-T	indel	SREBF2	frameshift_var	ENST0000036:c.1221_1227d	p.Ile407fs	0,4462	-
1-45271982-G-C	snv	TCTEX1D4	missense_vari:	ENST0000033:c.359C>G	p.Ala120Gly	0,4211	0,805
1-151748359-T-A	snv	TDRKH	missense_vari:	ENST0000036:c.1219A>T	p.Ser407Cys	0,4306	0,916
19-507636-G-A	snv	TPGS1	missense_vari:	ENST0000035:c.130G>A	p.Val44Met	0,44	0,987
10-135126315-G-A	snv	ZNF511	missense_vari:	ENST0000036:c.704G>A	p.Gly235Asp	0,4396	1
1-145558834-G-A	snv	ANKRD35	splice_acceptc	ENST0000035:c.454-1G>A	NA	0,6471	-
5-142152348-G-A	snv	ARHGAP26	start_lost	ENST0000037:c.3G>A	p.Met1?	0,4128	-
1-151016130-A-G	snv	BNIP1	missense_vari:	ENST0000029:c.532A>G	p.Ser178Gly	0,5	0,978
1-244715630-G-A	snv	C1orf101	stop_gained	ENST0000036:c.90G>A	p.Trp30*	0,5429	-
2-160637413-C-G	snv	CD302	missense_vari:	ENST0000025:c.275G>C	p.Gly92Ala	0,5197	1
1-153945918-C-T	snv	CREB3L4	missense_vari:	ENST0000027:c.875C>T	p.Ala292Val	0,625	0,999
7-111368102-C-A	snv	DOCK4	splice_region	ENST000004:c.*228G>T	NA	0,3333	-
19-13264523-G-T	snv	IER2	missense_vari:	ENST0000029:c.523G>T	p.Ala175Ser	0,3333	0,998
14-77951094-G-A	snv	ISM2	missense_vari:	ENST0000034:c.310C>T	p.Pro104Ser	0,3913	0,878
5-140720879-AGCCAG-A	indel	PCDHGA2	frameshift_var	ENST0000039:c.2343_2347d	p.Ser781fs	0,3662	-
6-137234626-A-G	snv	PEX7	missense_vari:	ENST0000031:c.934A>G	p.Lys312Glu	0,5316	0,568
7-106509420-C-G	snv	PIK3CG	missense_vari:	ENST0000035:c.1414C>G	p.Arg472Gly	0,5143	0,996
2-42281210-T-G	snv	PKDCC	missense_vari:	ENST0000029:c.797T>G	p.Leu266Arg	0,5	0,999
22-22890560-A-G	snv	PRAME	missense_vari:	ENST0000039:c.1459T>C	p.Cys487Arg	0,3571	0,998
9-79267444-G-A	snv	PRUNE2	missense_vari:	ENST0000022:c.304C>T	p.Leu102Phe	0,3	0,993
15-93586637-AAAAG-A	indel	RGMA	splice_region	ENST000003:c.*1587_*15	NA	0,4846	-
15-22318876-G-C	snv	RP11-69H14.6	splice_acceptc	ENST0000055:n.72-1G>C	NA	0,5	-
12-6085418-GAC-G	indel	VWF	frameshift_var	ENST0000026:c.7294_7295d	p.Val2432fs	0,5	-
2-169853220-G-C	snv	ABCB11	missense_vari:	ENST0000026:c.402C>G	p.Ile134Met	0,4407	0,987
10-49662209-G-C	snv	ARHGAP22	splice_region	ENST000002:c.793-5C>G	NA	0,3881	-
5-148997764-GC-TA	snv	ARHGEF37	missense_vari:	ENST0000033:c.684_685delC	p.GlnLeu228H	0,4697	0,98
12-122690902-C-G	snv	B3GNT4	missense_vari:	ENST0000032:c.104C>G	p.Ser35Trp	0,6226	0,465
7-158557366-A-T	snv	ESYT2	splice_donor_	ENST0000025:c.1245+2T>A	NA	0,625	-
16-30485543-G-T	snv	ITGAL	missense_vari:	ENST0000035:c.88G>T	p.Val30Leu	0,4744	0,629
19-55349335-G-C	snv	KIR2DS4	splice_region	ENST000003:c.370+5G>C	NA	0,5094	-
12-51442932-C-T	snv	LETMD1	missense_vari:	ENST0000026:c.238C>T	p.Pro80Ser	0,6207	1
17-72767835-C-CA	indel	NAT9	splice_region	ENST000005:c.*27dupT	NA	0,4706	-

5-1038369-G-A	snv	NKD2	missense_vari:ENST0000029:c.1237G>A	p.Asp413Asn	0,4167	0,951
10-79764641-G-A	snv	POLR3A	missense_vari:ENST0000037:c.2080C>T	p.Arg694Cys	0,4483	0,959
17-40557056-C-A	snv	PTRF	missense_vari:ENST0000035:c.822G>T	p.Met274Ile	0,5574	0,584
17-26076928-T-C	snv	RP1-66C13.3	splice_region ENST000005:n.428+8T>C	NA	0,3973	-
2-220329271-C-G	snv	SPEG	missense_vari:ENST0000031:c.2822C>G	p.Thr941Ser	0,36	0,974
2-220329286-A-T	snv	SPEG	missense_vari:ENST0000031:c.2837A>T	p.Asn946Ile	0,3438	1
17-61466699-A-T	snv	TANC2	missense_vari:ENST0000038:c.2623A>T	p.Asn875Tyr	0,5686	1
1-223991902-T-A	snv	TP53BP2	missense_vari:ENST0000034:c.623A>T	p.Gln208Leu	0,3704	0,576
1-32646902-C-T	snv	TXLNA	missense_vari:ENST0000037:c.229C>T	p.Arg77Cys	0,5135	0,998
8-196137-C-G	snv	ZNF596	missense_vari:ENST0000030:c.1290C>G	p.His430Gln	0,5086	0,994
19-20216083-C-A	snv	ZNF90	missense_vari:ENST0000041:c.184C>A	p.Pro62Thr	0,4625	0,612
19-56701680-G-C	snv	ZSCAN5B	missense_vari:ENST0000035:c.1004C>G	p.Pro335Arg	0,537	0,534
19-11512679-G-T	snv	RGL3	splice_region ENST000003:c.1484+8C>A	NA	0,3077	-
11-93462645-T-G	snv	KIAA1731	missense_vari:ENST0000032:c.7348T>G	p.Tyr2450Asp	0,4929	0,754
5-7520896-C-T	snv	ADCY2	missense_vari:ENST0000033:c.454C>T	p.Pro152Ser	0,3205	0,992
11-61735970-C-A	snv	AP003733.1	stop_gained ENST0000060:c.395C>A	p.Ser132*	0,4058	-
18-15325661-T-G	snv	AP005901.1	splice_region ENST000005(n.96A>C	NA	0,4471	-
15-83334211-C-A	snv	AP3B2	stop_gained ENST0000026:c.1969G>T	p.Glu657*	0,619	-
12-50344921-T-C	snv	AQP2	missense_vari:ENST0000019:c.308T>C	p.Leu103Pro	0,4722	0,967
22-19184002-T-C	snv	CLTCL1	missense_vari:ENST0000026:c.4039A>G	p.Lys1347Glu	0,4151	0,917
16-89662907-C-G	snv	CPNE7	missense_vari:ENST0000026:c.1780C>G	p.Leu594Val	0,4348	0,947
13-103518241-G-T	snv	ERCC5	stop_gained ENST0000035:c.2179G>T	p.Glu727*	0,5179	-
10-104180940-G-A	snv	FBXL15	splice_donor_ ENST0000022:c.53+1G>A	NA	0,4776	-
6-26199951-C-G	snv	HIST1H2BF	missense_vari:ENST0000035:c.165C>G	p.Ile55Met	0,3778	0,958
6-31795958-G-GT	indel	HSPA1B	frameshift_var ENST0000037:c.233dupT	p.Gly79fs	0,4865	-
14-107113890-AAACAT-A	indel	IGHV3-64	frameshift_var ENST0000045:c.200_204delA	p.Tyr67fs	0,6087	-
10-22019912-T-C	snv	MLLT10	missense_vari:ENST0000030:c.2147T>C	p.Ile716Thr	0,5122	0,996
6-51618038-C-G	snv	PKHD1	missense_vari:ENST0000034:c.8911G>C	p.Val2971Leu	0,4891	0,999
3-186921301-C-T	snv	RP11-208N14	splice_region ENST000003:n.671+7G>A	NA	0,5238	-
14-91444867-A-G	snv	RPS6KA5	splice_region_ ENST0000026:c.177T>C	p.Ala59Ala	0,438	-
2-27599569-G-C	snv	SNX17	missense_vari:ENST0000023:c.1396G>C	p.Gly466Arg	0,6667	0,996
4-186544452-G-C	snv	SORBS2	missense_vari:ENST0000028:c.2119C>G	p.Arg707Gly	0,5294	0,999
10-72541799-G-A	snv	TBATA	splice_region ENST000002:c.42-7C>T	NA	0,3171	-

1-36754896-C-T	snv	THRAP3	missense_vari:ENST0000035:c.1276C>T	p.His426Tyr	0,4034	0,857
19-36884353-G-C	snv	ZFP82	missense_vari:ENST0000039:c.889C>G	p.Leu297Val	0,458	0,998
5-142586764-C-A	snv	ARHGAP26	missense_vari:ENST0000027:c.1990C>A	p.Pro664Thr	0,3934	0,691
11-117160412-G-T	snv	BACE1	missense_vari:ENST0000031:c.1376C>A	p.Ala459Asp	0,4694	0,999
17-79058674-A-G	snv	BAIAP2	missense_vari:ENST0000032:c.260A>G	p.Gln87Arg	0,619	0,999
16-53263017-GA-G	indel	CHD9	splice_region ENST0000039:c.2286+6delA	NA	0,4672	-
12-122758678-A-G	snv	CLIP1	missense_vari:ENST0000030:c.3965T>C	p.Leu1322Pro	0,4625	1
X-13645316-G-C	snv	EGFL6	missense_vari:ENST0000036:c.1472G>C	p.Trp491Ser	0,3896	1
7-13946223-T-A	snv	ETV1	stop_gained ENST0000044:c.1006A>T	p.Arg336*	0,5286	-
2-70524507-C-T	snv	FAM136A	missense_vari:ENST0000003:c.331G>A	p.Val111Met	0,5128	0,688
12-95488447-C-T	snv	FGD6	stop_gained ENST0000034:c.3521G>A	p.Trp1174*	0,4068	-
16-67977904-G-A	snv	LCAT	missense_vari:ENST0000026:c.101C>T	p.Pro34Leu	0,6333	0,993
16-71674502-G-T	snv	MARVELD3	missense_vari:ENST0000029:c.805G>T	p.Gly269Cys	0,6522	0,998
15-56736662-C-A	snv	MNS1	missense_vari:ENST0000026:c.666G>T	p.Lys222Asn	0,4	1
20-49576022-T-C	snv	MOCS3	missense_vari:ENST0000024:c.643T>C	p.Tyr215His	0,4286	0,987
4-74719565-A-G	snv	PF4V1	missense_vari:ENST0000022:c.166A>G	p.Arg56Gly	0,5472	0,872
2-209223469-TACTC-T	indel	PIKFYVE	splice_region ENST000002(c.*3441_*34	NA	0,4239	-
3-48452438-T-G	snv	PLXNB1	missense_vari:ENST0000029:c.5255A>C	p.Asn1752Thr	0,6667	0,947
17-74276150-G-T	snv	QRICH2	missense_vari:ENST0000026:c.4214C>A	p.Pro1405Gln	0,4545	0,993
11-36597351-C-G	snv	RAG1	missense_vari:ENST0000029:c.2497C>G	p.Gln833Glu	0,4419	0,991
1-24861716-C-T	snv	RCAN3	missense_vari:ENST0000037:c.329C>T	p.Thr110Ile	0,4394	0,702
6-167184402-C-G	snv	RPS6KA2	splice_acceptc ENST0000050(c.124-1G>C	NA	0,425	-
15-44876743-A-C	snv	SPG11	missense_vari:ENST0000026:c.5135T>G	p.Met1712Arg	0,4783	0,774
7-23808651-C-A	snv	STK31	missense_vari:ENST0000035:c.1385C>A	p.Ala462Asp	0,5379	0,544
19-36499173-CGG-TGA	snv	SYNE4	missense_vari:ENST0000032:c.223_225delC	p.Pro75Ser	0,6667	0,986
1-161132467-C-T	snv	USP21	stop_gained ENST0000028:c.844C>T	p.Arg282*	0,551	-
19-42392910-G-T	snv	ARHGEF1	missense_vari:ENST0000033:c.244G>T	p.Ala82Ser	0,3939	0,999
19-42392911-C-T	snv	ARHGEF1	missense_vari:ENST0000033:c.245C>T	p.Ala82Val	0,4062	0,999
19-535836-G-C	snv	CDC34	splice_acceptc ENST0000021:c.178-1G>C		0,5161	-
1-86377102-T-G	snv	COL24A1	missense_vari:ENST0000037(c.2577A>C	p.Leu859Phe	0,4631	0,969
5-64181358-G-GA	indel	CWC27	frameshift_var ENST0000038:c.1033dupA	p.Arg345fs	0,4741	-
11-6567022-GC-G	indel	DNHD1	frameshift_var ENST0000025:c.4858delC	p.Leu1620fs	0,3846	-
17-71223312-C-T	snv	FAM104A	missense_vari:ENST0000040:c.313G>A	p.Asp105Asn	0,5085	0,999

11-92600004-C-T	snv	FAT3	missense_vari:ENST0000029:c.11756C>T	p.Ser3919Leu	0,3846	0,745
4-54325466-C-CTTTT	indel	FIP1L1	splice_acceptc ENST0000030:c.1416-3_1416		0,4074	-
4-54325464-TCC-T	indel	FIP1L1	splice_region ENST0000030:c.1416-4_1416	NA	0,3385	-
8-119209972-C-T	snv	SAMD12	splice_acceptc ENST0000040:c.464-1G>A	NA	0,5161	-
22-20783587-A-C	snv	SCARF2	missense_vari:ENST0000026:c.1480T>G	p.Cys494Gly	0,5238	0,999
15-42168484-T-G	snv	SPTBN5	splice_acceptc ENST0000032:c.3952-2A>C	NA	0,4286	-
2-210704049-G-C	snv	UNC80	missense_vari:ENST0000027:c.3130G>C	p.Asp1044His	0,4828	0,998
8-87460442-T-G	snv	WWP1	missense_vari:ENST0000026:c.2064T>G	p.Ser688Arg	0,4937	0,934
16-66997802-C-T	snv	CES3	missense_vari:ENST0000030:c.524C>T	p.Thr175Ile	0,6552	0,796
11-1902785-GC-G	indel	LSP1	frameshift_var ENST0000031:c.322delC	p.Gln108fs	0,5	-
10-45958752-A-T	snv	MARCH8	missense_vari:ENST0000045:c.935T>A	p.Val312Asp	0,5185	0,998
11-120308098-ATG-TTA	snv	ARHGEF12	splice_region ENST0000031:c.942+7_942	NA	0,5165	-
5-79054726-G-A	snv	CMYA5	splice_donor_ ENST0000044:c.11260+1G>A	NA	0,4948	-
16-11023421-CA-C	indel	DEXI	splice_region ENST0000033:c.*150-6delT	NA	0,3	-
1-94342964-T-C	snv	DNTTIP2	missense_vari:ENST0000035:c.527A>G	p.Gln176Arg	0,3824	0,988
19-1555686-G-A	snv	MEX3D	missense_vari:ENST0000038:c.1832C>T	p.Ala611Val	0,6923	0,995
1-148251901-G-T	snv	NBPF20	missense_vari:ENST0000036:c.13840C>A	p.Gln4614Lys	0,303	0,598
7-141899678-A-G	snv	RP11-1220K2.1	splice_acceptc ENST0000047:c.5049-2A>G	NA	0,38	-
12-113333684-T-C	snv	RPH3A	splice_region ENST0000033:c.1954+6T>C	NA	0,4902	-
7-39894553-T-C	snv	RWDD4P2	splice_region ENST000004:n.103A>G	NA	0,5254	-
12-56740298-C-T	snv	STAT2	missense_vari:ENST0000031:c.1972G>A	p.Glu658Lys	0,5806	0,999
15-84706544-TG-CA	snv	ADAMTSL3	missense_vari:ENST0000028:c.5062_5063d	p.Cys1688His	0,3864	1
1-49511310-G-C	snv	AGBL4	missense_vari:ENST0000037:c.540C>G	p.Ser180Arg	0,5037	0,434
12-96912805-G-A	snv	C12orf55	missense_vari:ENST0000029:c.898G>A	p.Val300Ile	0,3929	0,999
5-15928455-GC-AA	snv	FBXL7	missense_vari:ENST0000032:c.548_549delC	p.Gly183Glu	0,4141	0,998
11-47746113-C-A	snv	FNBP4	missense_vari:ENST0000026:c.2226G>T	p.Met742Ile	0,566	0,985
19-19257875-G-C	snv	MEF2B	missense_vari:ENST0000016:c.511C>G	p.Arg171Gly	0,4483	0,953
1-161180375-C-T	snv	NDUFS2	splice_region ENST0000033:c.867-6C>T	NA	0,5229	-
1-13910422-C-G	snv	PDPN	missense_vari:ENST0000029:c.122C>G	p.Pro41Arg	0,4615	0,985
3-135721164-A-C	snv	PPP2R3A	missense_vari:ENST0000026:c.824A>C	p.Glu275Ala	0,5185	0,76
11-20429490-C-T	snv	PRMT3	missense_vari:ENST0000033:c.805C>T	p.Leu269Phe	0,4533	0,984
20-25239866-T-C	snv	PYGB	splice_region ENST000002:c.244-7T>C	NA	0,4318	-
1-113460129-A-C	snv	SLC16A1	missense_vari:ENST0000036:c.899T>G	p.Phe300Cys	0,5238	0,992

8-145665415-A-C	snv	TONSL	missense_vari:ENST0000040:c.1469T>G	p.Leu490Arg	0,5873	0,472
10-104404538-G-A	snv	TRIM8	missense_vari:ENST0000030:c.164G>A	p.Cys55Tyr	0,4725	0,999
6-142510605-A-T	snv	VTA1	missense_vari:ENST0000036:c.280A>T	p.Ile94Phe	0,4886	1
3-113013576-C-G	snv	WDR52	missense_vari:ENST0000030:c.1140G>C	p.Lys380Asn	0,521	0,997
19-21991919-A-G	snv	ZNF43	missense_vari:ENST0000035:c.920T>C	p.Ile307Thr	0,36	0,992
19-21991923-T-A	snv	ZNF43	stop_gained ENST0000035:c.916A>T	p.Lys306*	0,3774	-
10-75561225-C-T	snv	ZSWIM8	missense_vari:ENST0000039:c.5477C>T	p.Thr182Ile	0,5849	0,997
1-115217397-G-C	snv	AMPD1	missense_vari:ENST0000035:c.1776C>G	p.Ile592Met	0,5	0,956
3-137964523-T-C	snv	ARMC8	splice_region ENST000004:c.*432T>C	NA	0,3933	-
6-44149065-G-A	snv	CAPN11	splice_region ENST000003:c.1938+8G>A	NA	0,5429	-
5-162869106-TAG-T	indel	CCNG1	frameshift_var ENST0000034:c.656_657delA	p.Glu219fs	0,4876	-
12-56333231-G-T	snv	DGKA	missense_vari:ENST0000033:c.627G>T	p.Arg209Ser	0,4062	0,968
1-98165090-AT-GC	snv	DPYD	missense_vari:ENST0000037:c.496_497delA	p.Met166Ala	0,4643	1
4-3446064-G-A	snv	HGFAC	missense_vari:ENST0000038:c.625G>A	p.Glu209Lys	0,5	0,974
11-66407365-T-TG	indel	RBM4	frameshift_var ENST0000031:c.187dupG	p.Val63fs	0,5586	-
15-45460186-G-C	snv	SHF	missense_vari:ENST0000029:c.1231C>G	p.His411Asp	0,4342	0,997
5-121739561-G-T	snv	SNCAIP	splice_donor_ ENST0000026:c.271+1G>T	NA	0,3525	-
3-120764348-G-A	snv	STXBP5L	missense_vari:ENST0000027:c.436G>A	p.Ala146Thr	0,5256	0,488
14-76201603-TC-T	indel	TLL5	frameshift_var ENST0000029:c.1254delC	p.Arg419fs	0,5256	-
19-55915700-T-C	snv	UBE2S	missense_vari:ENST0000026:c.298A>G	p.Lys100Glu	0,4038	0,999
19-36253198-A-C	snv	C19orf55	missense_vari:ENST0000030:c.481A>C	p.Thr161Pro	0,4766	0,939
19-49910914-A-T	snv	CCDC155	stop_gained ENST0000044:c.979A>T	p.Arg327*	0,4792	-
2-101009987-AC-A	indel	CHST10	frameshift_var ENST0000026:c.790delG	p.Val264fs	0,5179	-
17-40716564-G-C	snv	COASY	missense_vari:ENST0000039:c.1016G>C	p.Arg339Pro	0,4915	0,899
10-135340912-G-A	snv	CYP2E1	missense_vari:ENST0000025:c.13G>A	p.Gly5Arg	0,5854	0,964
7-37262215-C-G	snv	ELMO1	splice_region ENST000003:c.780+5G>C	NA	0,4821	-
7-76984590-C-G	snv	GSAP	missense_vari:ENST0000025:c.1278G>C	p.Lys426Asn	0,5	0,725
19-17448987-G-A	snv	GTPBP3	missense_vari:ENST0000032:c.224G>A	p.Arg75His	0,4605	1
7-86542483-G-C	snv	KIAA1324L	missense_vari:ENST0000029:c.1049C>G	p.Ser350Cys	0,4306	0,999
7-104702619-C-G	snv	KMT2E	missense_vari:ENST0000025:c.80C>G	p.Ser27Cys	0,438	0,999
2-142567943-A-C	snv	LRP1B	missense_vari:ENST0000038:c.110T>G	p.Phe37Cys	0,5742	0,997
22-31556050-C-G	snv	MIR3928	splice_region ENST000005:c.n.56G>C	NA	0,3844	-
2-1795656-T-C	snv	MYT1L	missense_vari:ENST0000039:c.3544A>G	p.Arg1182Gly	0,527	0,467

20-21376686-G-T	snv	NKX2-4	missense_vari:ENST0000035:c.928C>A	p.Pro310Thr	0,32	0,641
19-55495092-G-A	snv	NLRP2	missense_vari:ENST0000026:c.2017G>A	p.Glu673Lys	0,5	0,511
3-119526261-T-C	snv	NR1I2	missense_vari:ENST0000033:c.281T>C	p.Val94Ala	0,3878	0,998
15-96877632-C-T	snv	NR2F2	missense_vari:ENST0000039:c.770C>T	p.Ala257Val	0,5694	0,992
9-131747198-G-A	snv	NUP188	missense_vari:ENST0000037:c.1981G>A	p.Gly661Arg	0,5648	0,984
11-110070298-G-A	snv	RDX	splice_region ENST000004(c.*31+8C>T	NA	0,4571	-
5-9052139-C-T	snv	SEMA5A	splice_region_ ENST0000038:c.2691G>A	p.Glu897Glu	0,5517	-
19-17608216-C-G	snv	SLC27A1	missense_vari:ENST0000025:c.1149C>G	p.Ile383Met	0,4405	0,964
2-27595614-G-A	snv	SNX17	splice_region ENST000002:c.256+7G>A	NA	0,5373	-
22-41222568-A-C	snv	ST13	missense_vari:ENST0000021(c.1084T>G	p.Ser362Ala	0,5077	0,986
12-110348895-C-T	snv	TCHP	missense_vari:ENST0000031:c.907C>T	p.Leu303Phe	0,3898	0,998
6-32061089-TTAAAG-T	indel	TNXB	frameshift_var ENST0000047:c.2498_2502d	p.Thr833fs	0,3936	-
2-166785699-A-AT	indel	TTC21B	frameshift_var ENST0000024:c.1331dupA	p.Asn444fs	0,5083	-
21-43826473-G-A	snv	UBASH3A	splice_region ENST000002(c.167+3G>A	NA	0,3947	-
10-1123871-C-T	snv	WDR37	missense_vari:ENST0000026:c.163C>T	p.Arg55Cys	0,3426	0,983
3-93643083-C-T	snv	PROS1	splice_donor_ ENST0000034:c.355+1G>A		0,5045	-
22-36653123-C-T	snv	APOL1	splice_region ENST000003:c.93-6C>T	NA	0,5	-
1-3380187-T-C	snv	ARHGEF16	missense_vari:ENST0000037:c.539T>C	p.Leu180Pro	0,5686	0,836
4-114823449-G-C	snv	ARSJ	stop_gained ENST0000031:c.1781C>G	p.Ser594*	0,5789	-
17-58506718-G-A	snv	C17orf64	splice_region ENST000002(c.430-5G>A	NA	0,5128	-
8-22473033-C-A	snv	CCAR2	missense_vari:ENST0000030:c.1301C>A	p.Pro434His	0,35	1
17-73914051-G-A	snv	FBF1	missense_vari:ENST0000031:c.2302C>T	p.Arg768Trp	0,5417	0,972
4-843696-G-A	snv	GAK	missense_vari:ENST0000031:c.3818C>T	p.Ala1273Val	0,6552	0,806
2-238666112-T-C	snv	LRRFIP1	missense_vari:ENST0000030:c.1145T>C	p.Leu382Pro	0,5833	0,997
6-90405510-G-C	snv	MDN1	missense_vari:ENST0000036:c.9585C>G	p.Cys3195Trp	0,541	0,662
12-82752608-G-C	snv	METTL25	splice_region ENST000002(c.259+5G>C	NA	0,375	-
2-242757639-TG-AT	snv	NEU4	missense_vari:ENST0000032:c.759_760delT	p.AsnAla253Ly	0,4348	1
12-48499961-CA-C	indel	PFKM	splice_region ENST000005(c.-12delA	NA	0,4444	-
X-49142590-G-T	snv	PPP1R3F	missense_vari:ENST0000005:c.1438G>T	p.Gly480Cys	0,4545	0,996
5-120021869-C-A	snv	PRR16	missense_vari:ENST0000037:c.311C>A	p.Pro104Gln	0,5229	1
17-74151403-AG-A	indel	RNF157	splice_region ENST000002(c.1699-6delC	NA	0,4286	-
12-58180001-A-G	snv	TSFM	missense_vari:ENST0000032:c.287A>G	p.Lys96Arg	0,4615	0,91
13-110436371-G-T	snv	IRS2	missense_vari:ENST0000037:c.2030C>A	p.Pro677His	0,5385	0,99

3-52422605-C-T, 3-52425267-C-	snv, snv	DNAH1	missense_vari:ENST0000042(c.9343C>T, c.9p.Arg3115Trp, 0.5424, 0.421:0.996, 0.997
2-233404771-G-A, 2-233407702	snv, snv	CHNRG	missense_vari:ENST0000038(c.125G>A, c.55p.Arg42Gln, p. 0.5323, 0.492:0.707, 0.998
5-33683182-T-C	snv	ADAMTS12	missense_vari:ENST0000035:c.856A>G p.Ser286Gly 0,56 0,993
5-72800172-C-G	snv	BTF3	missense_vari:ENST0000033(c.386C>G p.Ser129Cys 0,4937 0,687
19-13410163-CT-C	indel	CACNA1A	frameshift_var ENST0000036(c.2283delA p.Glu762fs 0,44 -
16-80638352-A-G	snv	CDYL2	missense_vari:ENST0000056:c.1457T>C p.Leu486Pro 0,5965 0,998
15-43990833-C-G	snv	CKMT1A	splice_region ENST000004:c.1012-6C>G NA 0,5093 -
21-46906859-C-T	snv	COL18A1	missense_vari:ENST0000035(c.2326C>T p.Pro776Ser 0,4211 0,876
6-71004096-T-C	snv	COL9A1	missense_vari:ENST0000035:c.470A>G p.Tyr157Cys 0,5366 1
17-78402403-TCTG-T	indel	ENDOV	disruptive_infr ENST0000032:c.590_592delC p.Cys197del 0,4 -
1-11731368-G-A	snv	FBXO6	stop_gained ENST0000037(c.332G>A p.Trp111* 0,5 -
8-125076750-C-T	snv	FER1L6	missense_vari:ENST0000039(c.3491C>T p.Ser1164Phe 0,5 0,553
18-19079878-G-T	snv	GREB1L	missense_vari:ENST0000026(c.3253G>T p.Ala1085Ser 0,5729 0,567
12-66707768-C-A	snv	HELB	splice_region_ ENST0000024:c.1683C>A p.Val561Val 0,4 -
14-77951093-G-C	snv	ISM2	missense_vari:ENST0000034:c.311C>G p.Pro104Arg 0,413 0,979
12-4920313-T-C	snv	KCNA6	missense_vari:ENST0000028(c.1106T>C p.Leu369Ser 0,3654 0,999
9-5754886-T-A	snv	KIAA1432	missense_vari:ENST0000025:c.1648T>A p.Phe550Ile 0,4982 0,939
3-8590431-T-C	snv	LMCD1	missense_vari:ENST0000015:c.565T>C p.Tyr189His 0,5714 0,982
14-33684578-G-T	snv	NPAS3	missense_vari:ENST0000034:c.331G>T p.Asp111Tyr 0,4758 0,998
11-68359179-AAGAT-A	indel	PPP6R3	splice_region ENST000002(c.1676+6_16 NA 0,4479 -
2-44570953-T-TAGATG	indel	PREPL	frameshift_var ENST0000026(c.542_546dup p.Thr183fs 0,5341 -
2-191940954-T-G	snv	STAT4	missense_vari:ENST0000035:c.371A>C p.Gln124Pro 0,4945 0,987
14-64457820-T-C	snv	SYNE2	missense_vari:ENST0000034:c.2633T>C p.Ile878Thr 0,5814 0,894
4-165890878-C-A	snv	TRIM61	stop_gained ENST0000032(c.277G>T p.Glu93* 0,4737 -
19-6741078-T-C	snv	TRIP10	missense_vari:ENST0000031:c.82T>C p.Tyr28His 0,5068 1
2-179398281-G-C	snv	TTN	missense_vari:ENST0000034:c.76442C>G p.Pro25481Arg 0,4167 0,804
12-132394793-C-A	snv	ULK1	splice_region ENST000003:c.809-6C>A NA 0,4894 -
15-63852124-C-A	snv	USP3	missense_vari:ENST0000026(c.536C>A p.Ala179Glu 0,4483 1
15-67495939-G-C	snv	AAGAB	splice_region ENST000002(c.821-4C>G NA 0,4478 -
1-160136767-T-G	snv	ATP1A4	missense_vari:ENST0000036(c.1256T>G p.Phe419Cys 0,4578 1
6-33246306-TCGAG-T	indel	B3GALT4	frameshift_var ENST0000045:c.1112_1115d p.Arg371fs 0,5 -
1-85724613-G-A	snv	C1orf52	splice_region ENST000002(c.n.442+5C>T NA 0,5625 -
4-78085512-A-C	snv	CCNG2	missense_vari:ENST0000031(c.791A>C p.Asp264Ala 0,5676 0,51

11-125525175-A-G	snv	CHEK1	missense_vari:ENST0000027:c.1259A>G	p.Asp420Gly	0,4783	0,742
17-4802762-C-G	snv	CHRNE	splice_donor_ ENST0000029:c.1032+1G>C	NA	0,4583	-
7-99453266-T-G	snv	CYP3A43	missense_vari:ENST0000022:c.723T>G	p.Phe241Leu	0,55	0,551
15-83658755-C-G	snv	FAM103A1	missense_vari:ENST0000030:c.293C>G	p.Pro98Arg	0,5	0,608
6-35554830-T-C	snv	FKBP5	missense_vari:ENST0000035:c.821A>G	p.Lys274Arg	0,4264	0,674
6-35586953-A-C	snv	FKBP5	missense_vari:ENST0000035:c.428T>G	p.Phe143Cys	0,4286	0,797
6-35554830-T-C, 6-35586953-A-	snv, snv	FKBP5	missense_vari:ENST0000035:c.821A>G, c.428T>G	p.Lys274Arg, p.Phe143Cys	0,4264, 0,4286	0,674, 0,797
11-62398086-G-A	snv	GANAB	missense_vari:ENST0000034:c.1439C>T	p.Ser480Phe	0,587	0,516
2-240036762-A-C	snv	HDAC4	missense_vari:ENST0000034:c.1763T>G	p.Leu588Arg	0,3721	0,934
12-54676916-AGTG-A	indel	HNRNPA1	disruptive_infr ENST0000034:c.810_812delT	p.Gly271del	0,4026	-
18-59925829-G-A	snv	KIAA1468	missense_vari:ENST0000025:c.2122G>A	p.Ala708Thr	0,4966	0,996
21-46057429-G-T	snv	KRTAP10-10	missense_vari:ENST0000038:c.95G>T	p.Cys32Phe	0,3333	0,831
19-7593098-C-T	snv	MCOLN1	stop_gained ENST0000026:c.832C>T	p.Gln278*	0,4355	-
17-37565593-C-A	snv	MED1	missense_vari:ENST0000030:c.2881G>T	p.Gly961Trp	0,4878	0,973
7-8474393-C-A	snv	NXPH1	splice_region ENST0000004:c.-111+8C>A	NA	0,3333	-
11-65393514-A-G	snv	PCNXL3	missense_vari:ENST0000035:c.3368A>G	p.Tyr1123Cys	0,5323	0,827
11-65393514-A-G, 11-65403969	snv, snv	PCNXL3	missense_vari:ENST0000035:c.3368A>G, c.519G>T	p.Tyr1123Cys, p.Tyr519Cys	0,5323, 0,3333	0,827, 0,689
10-103990272-C-T	snv	PITX3	stop_retained_ ENST0000037:c.908G>A	p.Ter303Ter	0,537	-
19-51920622-G-T	snv	SIGLEC10	stop_gained ENST0000033:c.135C>A	p.Tyr45*	0,55	-
9-4662000-C-G	snv	SPATA6L	missense_vari:ENST0000038:c.76G>C	p.Asp26His	0,3947	0,996
5-35727926-G-A	snv	SPEF2	splice_donor_ ENST0000035:c.3063+1G>A	NA	0,5625	-
9-136198736-G-A	snv	SURF6	missense_vari:ENST0000037:c.1055C>T	p.Pro352Leu	0,625	0,726
14-64490987-CT-C	indel	SYNE2	frameshift_var ENST0000034:c.5652delT	p.Glu1885fs	0,5	-
7-100225899-A-C	snv	TFR2	missense_vari:ENST0000022:c.1421T>G	p.Ile474Ser	0,4222	0,842
20-57599769-AG-A	indel	TUBB1	frameshift_var ENST0000021:c.1288delG	p.Ala430fs	0,4722	-
22-41278005-GC-G	indel	XPNPEP3	frameshift_var ENST0000035:c.415delC	p.Leu139fs	0,52	-
1-154987482-G-A	snv	ZBTB7B	missense_vari:ENST0000029:c.346G>A	p.Ala116Thr	0,5385	0,776
1-87368961-TA-T	indel	SEPT15	splice_donor_ ENST0000033:c.243+2delT	NA	0,3929	-
1-87368963-C-G	snv	SEPT15	splice_donor_ ENST0000033:c.243+1G>C	NA	0,386	-
1-87368959-A-ATTTGGTTTCA,	indel	SEPT15	splice_region ENST0000003:c.243+4_243delT	NA	0,3818	-
5-56777621-G-A	snv	ACTBL2	missense_vari:ENST0000042:c.914C>T	p.Thr305Ile	0,4301	0,869
1-19712212-T-C	snv	CAPZB	splice_region ENST0000004:c.9+3A>G	NA	0,4393	-
9-90254284-C-G	snv	DAPK1	missense_vari:ENST0000035:c.439C>G	p.Leu147Val	0,4153	0,727

22-39177010-G-A	snv	DNAL4	missense_vari:ENST0000021:c.74C>T	p.Ser25Leu	0,5584	0,612
1-16384993-C-G	snv	FAM131C	missense_vari:ENST0000037:c.782G>C	p.Gly261Ala	0,4531	0,727
2-186661119-A-G	snv	FSIP2	missense_vari:ENST0000034:c.9523A>G	p.Ile3175Val	0,4962	0,682
2-186664870-C-T	snv	FSIP2	missense_vari:ENST0000034:c.11104C>T	p.His3702Tyr	0,454	0,611
12-7842481-C-T	snv	GDF3	missense_vari:ENST0000032:c.1088G>A	p.Cys363Tyr	0,487	1
7-37780813-C-T	snv	GPR141	missense_vari:ENST0000033:c.818C>T	p.Thr273Ile	0,4318	1
X-19025439-C-T	snv	GPR64	missense_vari:ENST0000035:c.1555G>A	p.Val519Ile	1	0,789
2-213921458-CA-C	indel	IKZF2	frameshift_var ENST0000043:c.416delT	p.Val139fs	0,4914	-
6-36452587-G-T	snv	KCTD20	missense_vari:ENST0000037:c.953G>T	p.Arg318Leu	0,3832	0,578
4-55599266-A-G	snv	KIT	missense_vari:ENST0000028:c.2392A>G	p.Ile798Val	0,4552	0,997
17-45913026-C-T	snv	LRRC46	splice_region ENST000002:c.273-6C>T	NA	0,4068	-
6-32165365-A-AC	indel	NOTCH4	frameshift_var ENST0000037:c.4762dupG	p.Val1588fs	0,4945	-
15-31776700-G-C	snv	OTUD7A	missense_vari:ENST0000030:c.1578C>G	p.Ile526Met	0,4493	0,994
12-27951735-G-T	snv	RP11-860B13	splice_region ENST000005:c.30C>A	NA	0,377	-
13-23906787-G-T	snv	SACS	missense_vari:ENST0000038:c.11228C>A	p.Pro3743His	0,4621	0,999
15-44091545-C-G	snv	SERINC4	missense_vari:ENST0000029:c.242G>C	p.Arg81Thr	0,4607	0,64
X-9905229-G-A	snv	SHROOM2	missense_vari:ENST0000038:c.3643G>A	p.Val1215Met	1	0,988
11-124508483-A-C	snv	SIAE	stop_gained ENST0000026:c.1275T>G	p.Tyr425*	0,4494	-
9-35606002-C-T	snv	TESK1	stop_gained ENST0000033:c.241C>T	p.Gln81*	0,5172	-
6-80715544-C-A	snv	TTK	splice_region ENST000002:c.-14-3C>A	NA	0,449	-
1-229773855-GC-TT	snv	URB2	missense_vari:ENST0000025:c.3495_3496d	p.LeuPro1165I	0,4725	0,997
9-136640054-T-C	snv	VAV2	splice_region ENST000003:c.2135+3A>G	NA	0,52	-
10-101604087-G-A	snv	ABCC2	stop_gained ENST0000037:c.3852G>A	p.Trp1284*	0,5091	-
11-66326820-C-T	snv	ACTN3	missense_vari:ENST0000050:c.1519C>T	p.Arg507Cys	0,5567	1
1-111998816-A-G	snv	ATP5F1	missense_vari:ENST0000036:c.332A>G	p.Tyr111Cys	0,4571	0,991
1-911914-G-A	snv	C1orf170	missense_vari:ENST0000034:c.1898C>T	p.Thr633Met	0,4667	0,997
12-91348092-C-CA	indel	CCER1	frameshift_var ENST0000035:c.427dupT	p.Trp143fs	0,5	-
1-27706007-G-A	snv	CD164L2	splice_region ENST000003:c.519-8C>T	NA	0,5618	-
19-43026295-C-T	snv	CEACAM1	missense_vari:ENST0000016:c.484G>A	p.Ala162Thr	0,4977	0,85
8-27328711-C-G	snv	CHRNA2	splice_region ENST000002:c.-136G>C	NA	0,3333	-
1-86954854-G-C	snv	CLCA1	splice_donor_ ENST0000023:c.1357+1G>C	NA	0,5441	-
7-7571517-T-C	snv	COL28A1	missense_vari:ENST0000039:c.143A>G	p.Asp48Gly	0,5263	1
13-46632327-TC-T	indel	CPB2	frameshift_var ENST0000018:c.985delG	p.Asp329fs	0,4623	-

18-28720216-T-TGACA	indel	DSC1	frameshift_var	ENST0000025'	c.1305_1308d	p.Ile437fs	0,4674	-
14-89206880-G-A	snv	EML5	stop_gained	ENST0000035'	c.562C>T	p.Arg188*	0,4421	-
15-44175900-C-T	snv	FRMD5	splice_donor_	ENST0000040'	c.1135+1G>A		0,5312	-
10-30663257-C-T	snv	GOLGA2P6	splice_region	ENST0000034'	n.59G>A	NA	0,4419	-
12-133360805-A-G	snv	GOLGA3	missense_vari:	ENST0000020'	c.3212T>C	p.Leu1071Pro	0,451	0,851
7-86468344-C-T	snv	GRM3	missense_vari:	ENST0000036'	c.1514C>T	p.Pro505Leu	0,5227	1
12-124135573-C-G	snv	GTF2H3	missense_vari:	ENST0000022'	c.274C>G	p.Leu92Val	0,4159	0,999
2-234749695-G-T	snv	HJURP	stop_gained	ENST0000041'	c.1731C>A	p.Tyr577*	0,5	-
13-74518161-G-A	snv	KLF12	missense_vari:	ENST0000037'	c.80C>T	p.Pro27Leu	0,4444	0,47
12-53876867-G-A	snv	MAP3K12	missense_vari:	ENST0000026'	c.1621C>T	p.Arg541Cys	0,6038	0,999
17-2381186-A-G	snv	METTL16	splice_region	ENST000002'	c.129-7T>C	NA	0,5143	-
19-2046241-G-T	snv	MKMK2	missense_vari:	ENST0000025'	c.283C>A	p.His95Asn	0,3614	0,635
19-15582919-C-T	snv	PGLYRP2	splice_region	ENST000002'	c.1133-8G>A	NA	0,6471	-
X-24742562-G-C	snv	POLA1	missense_vari:	ENST0000037'	c.1293G>C	p.Lys431Asn	0,4599	0,58
9-98229692-G-A	snv	PTCH1	missense_vari:	ENST0000033'	c.2266C>T	p.Leu756Phe	0,4353	0,668
1-178421789-T-C	snv	RASAL2	splice_donor_	ENST0000036'	c.2009+2T>C	NA	0,461	-
17-695072-C-G	snv	RNMTL1	stop_gained	ENST0000030'	c.1026C>G	p.Tyr342*	0,5823	-
18-29340189-G-GA	indel	SLC25A52	frameshift_var	ENST0000026'	c.465dupT	p.Gln156fs	0,4789	-
3-160129860-CAGAGG-C	indel	SMC4	frameshift_var	ENST0000034'	c.845_849delC	p.Gly282fs	0,4516	-
3-113218378-C-T	snv	SPICE1	missense_vari:	ENST0000029'	c.199G>A	p.Glu67Lys	0,4479	0,999
16-19474689-G-C	snv	TMC5	splice_region_	ENST0000021'	c.498G>C	p.Arg166Arg	0,3789	-
20-49457152-T-G	snv	TMSB4XP6	splice_region	ENST000004'	n.135A>C	NA	0,4763	-
17-7464312-C-T	snv	TNFSF13	splice_region	ENST000003'	c.738-4C>T	NA	0,4959	-
3-36933832-C-T	snv	TRANK1	splice_acceptc	ENST0000030'	c.-1146-1G>A	NA	0,5462	-
X-123041027-C-A	snv	XIAP	missense_vari:	ENST0000035'	c.1490C>A	p.Ser497Tyr	0,45	0,984
7-100358120-G-C	snv	ZAN	missense_vari:	ENST0000034'	c.3803G>C	p.Arg1268Thr	0,4966	0,842
6-28116539-C-G	snv	ZKSCAN8	missense_vari:	ENST0000033'	c.354C>G	p.Asn118Lys	0,5556	0,599
21-15730198-A-G	snv	ABCC13	splice_region	ENST000004'	n.3220+3A>C	NA	0,5745	-
10-61833450-G-GTTC	indel	ANK3	conservative_i	ENST0000028'	c.7186_7188d	p.Glu2396dup	0,4242	-
17-80915296-C-T	snv	B3GNTL1	stop_gained	ENST0000032'	c.800G>A	p.Trp267*	0,3824	-
1-208062848-C-G	snv	CD34	missense_vari:	ENST0000031'	c.716G>C	p.Arg239Thr	0,507	0,583
20-48808233-C-G	snv	CEBPB	missense_vari:	ENST0000030'	c.663C>G	p.Ser221Arg	0,3636	0,473
21-46897383-T-TG	indel	COL18A1	frameshift_var	ENST0000035'	c.1532dupG	p.Arg512fs	0,4016	-

4-52729645-A-T	snv	DCUN1D4	missense_vari:ENST0000033:c.68A>T	p.His23Leu	0,5062	0,998
9-95773549-A-C	snv	FGD3	missense_vari:ENST0000033:c.1030A>C	p.Lys344Gln	0,5044	0,998
20-3641281-C-T	snv	GFRA4	stop_gained ENST0000047:c.540G>A	p.Trp180*	0,3913	0,993
12-54757544-GCCA-G	indel	GPR84	disruptive_infr ENST0000026:c.89_91delTG	p.Val30del	0,4516	-
6-73843193-C-T	snv	KCNQ5	stop_gained ENST0000034:c.1354C>T	p.Gln452*	0,4681	-
8-95556152-C-A	snv	KIAA1429	missense_vari:ENST0000029:c.82G>T	p.Val28Leu	0,5	0,99
2-26203993-G-T	snv	KIF3C	missense_vari:ENST0000026:c.794C>A	p.Ala265Asp	0,5429	0,958
5-54522499-C-A	snv	MCIDAS	splice_region ENST0000005:c.218-4G>T	NA	0,6957	-
16-814046-G-A	snv	MSLN	missense_vari:ENST0000038:c.203G>A	p.Gly68Asp	0,6026	0,996
6-49426993-T-G	snv	MUT	missense_vari:ENST0000027:c.187A>C	p.Thr63Pro	0,5342	0,992
13-109777579-G-T	snv	MYO16	missense_vari:ENST0000035:c.3589G>T	p.Asp1197Tyr	0,4382	0,991
1-236154247-C-G	snv	NID1	missense_vari:ENST0000026:c.2867G>C	p.Arg956Pro	0,3143	0,562
3-136002731-C-G	snv	PCCB	missense_vari:ENST0000025:c.596C>G	p.Pro199Arg	0,5	1
5-149212760-C-T	snv	PPARGC1B	missense_vari:ENST0000030:c.1124C>T	p.Pro375Leu	0,5758	0,958
X-12841282-A-T	snv	PRPS2	splice_region ENST0000004:c.*367A>T	NA	0,42	-
16-67961354-T-C	snv	PSKH1	missense_vari:ENST0000029:c.1084T>C	p.Ser362Pro	0,5814	0,637
9-116612968-T-G	snv	RP11-534I8.1	splice_region ENST0000004:n.945A>C	NA	0,6667	-
6-74320139-G-T	snv	SLC17A5	missense_vari:ENST0000035:c.1243C>A	p.Leu415Met	0,4632	0,803
6-96990779-G-C	snv	UFL1	missense_vari:ENST0000036:c.1289G>C	p.Gly430Ala	0,4433	0,905
22-29444471-ACAT-A	indel	ZNRF3	disruptive_infr ENST0000033:c.711_713delC	p.Ile238del	0,3824	-
16-87678418-G-A	snv	JPH3	missense_var ENST0000028:c.937G>A	p.Gly313Ser	0,9915	1
2-100453961-CT-AC	snv	AFF3	missense_vari:ENST0000031:c.898_899delA	p.Ser300Val	0,5353	0,998
4-145985843-T-G	snv	ANAPC10	splice_region_ ENST0000030:c.208A>C	p.Arg70Arg	0,5	-
1-45190271-TG-T	indel	C1orf228	frameshift_var ENST0000045:c.983delG	p.Gly328fs	0,5238	-
8-22458387-C-T	snv	C8orf58	splice_region ENST0000028:c.41-8C>T	NA	0,4583	-
17-63739286-C-T	snv	CEP112	missense_vari:ENST0000031:c.275G>A	p.Ser92Asn	0,5063	0,697
17-40714906-A-G	snv	COASY	missense_vari:ENST0000039:c.266A>G	p.Asn89Ser	0,4932	0,997
14-31355483-A-T	snv	COCH	missense_vari:ENST0000021:c.1442A>T	p.Asp481Val	0,4722	1
9-124528916-T-C	snv	DAB2IP	missense_vari:ENST0000025:c.1520T>C	p.Leu507Pro	0,4118	1
9-90301580-C-A	snv	DAPK1	missense_vari:ENST0000035:c.2339C>A	p.Pro780Gln	0,5	0,999
5-172336768-A-G	snv	ERGIC1	splice_region ENST0000003:c.115+4A>G	NA	0,5763	-
2-132181375-G-C	snv	GNAQP1	splice_region ENST0000004:n.1066C>G	NA	0,3	-
4-123168488-C-A	snv	KIAA1109	missense_vari:ENST0000026:c.5488C>A	p.Gln1830Lys	0,4714	0,977

18-13643418-G-C	snv	LDLRAD4	splice_region	ENST000003	c.390+7G>C	NA	0,3	-
3-189690661-A-G	snv	LEPREL1	splice_donor	ENST0000031	c.1699+2T>C	NA	0,4375	-
9-123374673-C-T	snv	MEGF9	splice_donor	ENST0000037	c.1087+1G>A	NA	0,4881	-
6-36940476-C-G	snv	MTCH1	splice_region	ENST000003	c.855+3G>C	NA	0,5368	-
12-57113813-G-T	snv	NACA	missense_vari	ENST0000045	c.1501C>A	p.Leu501Met	0,5231	0,975
6-138753035-A-T	snv	NHSL1	missense_vari	ENST0000034	c.2447T>A	p.Val816Asp	0,3871	0,565
7-156752945-G-A	snv	NOM1	splice_region	ENST000004	n.256G>A	NA	0,5686	-
7-102040073-A-G	snv	PRKRIP1	missense_vari	ENST0000035	c.170A>G	p.Tyr57Cys	0,45	0,971
12-130921719-C-A	snv	RIMBP2	missense_vari	ENST0000026	c.1723G>T	p.Asp575Tyr	0,5172	1
11-65487855-C-T	snv	RNASEH2C	missense_vari	ENST0000030	c.206G>A	p.Arg69Gln	0,4188	0,99
13-114152828-A-G	snv	TMCO3	missense_vari	ENST0000037	c.616A>G	p.Asn206Asp	0,5114	0,888
11-8661868-G-T	snv	TRIM66	missense_vari	ENST0000029	c.1619C>A	p.Pro540His	0,449	0,999
9-88968104-G-A	snv	ZCCHC6	missense_vari	ENST0000037	c.11C>T	p.Thr4Ile	0,4	0,617
7-45717862-A-G	snv	ADCY1	missense_vari	ENST0000029	c.1898A>G	p.Gln633Arg	0,4231	0,871
14-78170731-A-C	snv	ALKBH1	stop_gained	ENST0000021	c.273T>G	p.Tyr91*	0,486	-
4-113189548-GATCA-G	indel	AP1AR	frameshift_var	ENST0000027	c.894_897delT	p.Gln299fs	0,4532	-
2-198641770-CAAAAGATCATAC	indel	BOLL	frameshift_var	ENST0000032	c.306_312+12	p.Gln103fs	0,474	-
15-43023408-C-T	snv	CDAN1	splice_donor	ENST0000035	c.1860+1G>A	NA	0,6311	-
1-87031696-G-A	snv	CLCA4	missense_vari	ENST0000026	c.86G>A	p.Ser29Asn	0,4878	0,866
8-2818689-T-C	snv	CSMD1	missense_vari	ENST0000033	c.7927A>G	p.Ile2643Val	0,4	1
19-58870564-A-G	snv	CTD-2619J13	splice_region	ENST000005	n.201T>C	NA	0,5	-
1-47181972-C-A	snv	EFCAB14	missense_vari	ENST0000037	c.329G>T	p.Arg110Leu	0,4286	0,906
4-139981655-G-A	snv	ELF2	missense_vari	ENST0000026	c.944C>T	p.Ala315Val	0,4262	0,557
19-48525527-T-TGTG	indel	ELSPBP1	conservative_i	ENST0000033	c.616_618dup	p.Val206dup	0,4862	-
12-247817-G-C	snv	IQSEC3	missense_vari	ENST0000032	c.1288G>C	p.Glu430Gln	0,4426	0,949
1-33235972-TC-T	indel	KIAA1522	frameshift_var	ENST0000037	c.1017delC	p.Val340fs	0,4783	-
10-85982133-G-T	snv	LRIT2	missense_vari	ENST0000037	c.1196C>A	p.Ala399Glu	0,5185	0,638
20-5974343-T-A	snv	MCM8	splice_donor	ENST0000026	c.2382+2T>A	NA	0,4805	-
20-5967973-G-A, 20-5974343-T-	snv, snv	MCM8	missense_vari	ENST0000026	c.2161G>A, c.2	p.Ala721Thr,	0,4252, 0,4805	1, -
7-141780612-C-T	snv	MGAM	missense_var	ENST000004	c.5869C>T	p.Arg1957Trp	0,9583	0,904
11-7982080-A-C	snv	NLRP10	missense_vari	ENST0000032	c.1079T>G	p.Val360Gly	0,3836	0,698
9-137968946-T-G	snv	OLFM1	missense_vari	ENST0000037	c.385T>G	p.Trp129Gly	0,5096	0,504
11-55406353-C-T	snv	OR4P4	missense_var	ENST000003	c.520C>T	p.His174Tyr	0,9889	0,994

19-49362155-T-TG	indel	PLEKHA4	frameshift_var ENST0000026:c.933dupC	p.Arg312fs	0,3256	-
11-63519999-T-C	snv	RTN3	missense_vari:ENST0000033:c.2702T>C	p.Ile901Thr	0,3735	0,994
3-15311325-ACG-GCA	snv	SH3BP5	missense_vari:ENST0000038:c.388_390delC	p.Arg130Cys	0,5	0,985
19-51768617-C-T	snv	SIGLECL1	splice_region ENST000003:c.23-5C>T	NA	0,4627	-
17-31324734-G-C	snv	SPACA3	missense_vari:ENST0000026:c.586G>C	p.Ala196Pro	0,5789	0,995
2-27263017-C-T	snv	TMEM214	missense_vari:ENST0000023:c.1742C>T	p.Ala581Val	0,4364	0,983
12-110240888-T-C	snv	TRPV4	missense_vari:ENST0000026:c.620A>G	p.Asn207Ser	0,5532	0,986
7-157060377-C-G	snv	UBE3C	missense_vari:ENST0000034:c.3180C>G	p.Phe1060Leu	0,5823	0,968
1-216370067-A-G	snv	USH2A	splice_region ENST000003(c.4082-3T>C	NA	0,5391	-

pLI	Genic Constrai	RVIS (%)	LOEUF
0,600	0,840	5,269	0,213
0,508	7,353	14,575	0,214
0,508	7,353	14,575	0,214
1,000	0,209	1,623	0,033
0,600	0,840	5,269	0,213
0,600	0,840	5,269	0,213
1,000	1,108	1,887	0,064
0,508	7,353	14,575	0,214
1,000	23,962	0,186	0,048
0,508	7,353	14,575	0,214
NA	NA	100,000	NA
0,000	88,812	98,563	0,145
0,000	5,481	7,341	0,869
0,701	12,417	2,336	0,218
0,016	59,720	24,487	0,153
0,000	97,284	73,226	1,360
0,787	27,281	29,110	0,167
0,004	40,390	44,995	0,305
0,001	61,728	35,904	0,391
0,000	70,091	94,330	0,482
0,000	70,091	94,330	0,482
0,072	42,491	41,965	0,518
NA	NA	80,860	0,156
0,000	89,306	92,600	0,884
0,711	86,316	61,740	0,157
0,004	10,156	61,984	0,368
0,856	37,366	47,175	0,158
0,815	34,305	24,467	0,864
1,000	21,723	95,093	1,360
0,000	31,962	58,143	0,935
0,000	99,715	85,855	0,864

0,000	89,608	93,470	1,470
0,032	34,529	76,100	0,159
0,000	70,255	63,089	0,878
0,000	97,800	NA	0,159
0,489	79,309	12,923	0,879
0,000	34,815	43,851	0,890
0,000	80,373	98,407	0,696
0,873	12,379	6,745	0,159
0,000	96,329	89,814	0,651
0,000	42,678	32,991	0,484
1,000	13,679	3,001	0,160
NA	NA	96,119	0,162
0,970	25,970	25,181	2,208
0,000	80,796	74,106	0,907
0,012	22,475	59,150	0,911
1,000	25,449	3,392	0,163
0,043	79,150	43,470	0,333
0,000	86,908	99,267	0,911
0,724	62,392	30,655	0,158
0,060	85,811	94,848	0,344
NA	NA	NA	0,453
0,000	88,219	97,537	0,456
0,990	7,034	6,256	0,457
-	NA	NA	-
0,842	8,697	34,819	0,457
0,842	15,643	45,816	0,697
1,000	16,395	2,278	0,688
0,993	90,925	31,193	0,160
0,000	99,506	99,216	0,866
0,000	98,217	19,736	0,703
0,000	36,104	8,690	0,458
0,988	26,941	11,251	0,459
0,949	25,267	78,651	0,150

0,008	28,203	21,105	0,472
0,000	98,409	81,652	0,691
0,022	59,166	52,434	0,472
0,991	7,879	14,174	1,938
0,092	57,388	56,696	0,353
0,000	58,178	35,044	0,590
0,741	39,396	19,531	0,184
-	NA	NA	-
0,978	38,250	31,887	0,000
0,047	69,997	48,416	0,473
1,000	1,416	1,896	0,476
0,000	96,768	69,394	0,708
0,000	67,259	48,827	0,393
0,000	67,259	48,827	0,395
1,000	0,132	1,984	0,402
0,004	2,080	1,691	0,404
0,991	58,321	86,520	0,411
0,001	14,562	17,283	1,067
NA	NA	NA	0,417
0,795	17,953	36,764	0,423
0,352	37,421	55,797	0,235
0,000	11,973	38,319	0,708
0,000	70,804	88,446	0,423
0,000	81,783	77,478	0,423
0,016	26,787	21,447	0,708
0,001	44,181	62,444	0,885
0,000	22,645	12,102	0,427
0,000	44,988	37,527	0,429
0,000	37,213	32,473	0,710
0,704	23,989	17,146	0,434
0,000	61,015	78,729	0,439
0,001	35,462	62,366	0,703
0,996	61,059	21,632	0,440

0,996	61,059	21,632	0,440
0,996	61,059	21,632	0,118
0,209	18,623	NA	0,377
0,007	42,722	57,165	0,371
0,003	15,051	NA	0,444
0,014	39,868	58,426	0,453
0,000	48,527	93,754	0,688
0,999	14,848	10,479	0,222
0,000	42,365	78,719	0,888
0,000	63,868	49,599	1,013
0,009	81,339	41,945	1,015
0,000	91,171	77,986	0,663
0,999	34,820	11,613	0,171
0,681	34,272	54,917	0,973
0,000	72,593	90,420	0,224
0,000	28,598	74,330	0,224
0,000	70,008	29,110	0,228
0,564	17,021	16,979	0,766
0,000	51,100	67,028	0,708
0,001	93,838	54,604	0,523
0,000	93,503	98,348	0,229
0,011	52,472	53,891	0,553
NA	NA	NA	0,230
0,000	30,447	93,656	0,233
0,000	69,888	51,593	0,532
0,001	61,811	77,869	0,463
0,000	81,421	93,333	1,003
0,000	97,992	37,243	1,077
0,008	35,830	7,537	0,307
0,430	16,905	5,885	0,224
-	NA	NA	-
0,794	45,536	39,765	0,146
0,081	71,567	46,882	0,369

0,000	90,348	85,210	0,808
0,000	22,228	2,346	0,569
0,021	3,418	42,307	0,609
-	NA	NA	-
1,000	0,494	47,380	0,167
1,000	0,494	47,380	0,167
1,000	26,974	0,371	0,050
0,002	36,713	13,793	0,319
0,996	30,052	36,676	0,000
0,000	99,682	43,011	1,082
0,000	99,605	50,674	1,138
0,000	97,706	96,882	1,490
0,000	79,007	93,441	0,967
0,003	67,995	NA	1,856
1,000	0,938	5,318	0,026
NA	NA	NA	NA
-	NA	NA	-
0,990	7,034	6,256	0,140
0,000	27,188	34,330	1,067
0,000	89,333	98,475	0,890
0,000	89,185	59,003	0,980
0,000	78,826	92,678	0,434
0,002	6,288	57,810	0,947
0,000	64,582	24,702	2,592
NA	NA	NA	NA
NA	NA	NA	#N/A
1,000	51,654	3,089	0,101
0,000	98,370	17,351	0,464
-	NA	NA	-
1,000	25,904	41,017	0,035
0,686	43,715	23,011	0,190
0,089	53,026	37,576	0,259
0,000	77,449	92,854	0,919

1,000	16,735	8,895	0,025
0,052	28,395	29,316	0,321
0,999	14,848	10,479	0,184
0,944	11,281	26,755	0,185
0,464	17,471	11,212	0,953
1,000	16,241	0,528	0,112
0,968	32,132	6,706	0,185
0,000	51,380	92,633	0,187
0,997	67,731	27,468	0,188
0,001	77,169	63,021	1,085
0,995	78,573	51,525	0,190
0,496	30,299	50,792	0,792
0,000	53,388	17,791	0,798
0,000	93,350	46,911	0,193
0,000	16,883	42,424	0,194
0,007	60,428	47,996	0,195
0,980	27,786	1,212	0,198
0,850	9,021	64,301	0,986
0,000	63,523	91,672	0,799
0,002	56,461	12,483	0,803
0,003	53,492	67,634	0,589
0,085	12,971	4,624	0,197
0,000	98,727	1,750	0,197
0,233	91,177	88,172	0,198
0,000	76,823	94,633	0,808
0,075	23,150	32,835	0,263
0,909	4,236	15,836	0,183
0,909	4,236	15,836	0,183
0,560	23,896	41,672	0,156
0,000	98,195	77,322	0,652
0,000	69,136	31,916	0,179
0,000	79,610	NA	0,810
0,612	69,119	56,461	0,179

1,000	51,292	NA	0,960
0,601	5,427	8,084	0,211
0,601	5,427	8,084	0,211
0,001	76,647	50,743	0,180
NA	NA	49,462	0,183
0,000	99,479	99,902	0,183
0,140	45,224	NA	0,284
0,957	16,922	8,221	0,183
0,000	70,480	95,161	0,708
0,260	74,365	65,376	0,980
0,000	47,610	55,357	0,175
1,000	9,915	4,633	0,102
0,000	98,305	99,775	0,169
0,454	25,465	43,050	0,000
0,000	86,716	40,518	1,077
NA	NA	NA	0,985
0,000	15,841	NA	1,597
0,029	62,700	NA	0,831
0,739	40,318	61,564	0,200
-	NA	NA	-
0,041	23,945	17,234	0,175
0,000	78,167	82,952	0,402
0,000	68,181	NA	0,883
0,000	96,335	NA	0,620
0,200	7,364	24,233	0,277
1,000	36,576	25,200	0,027
0,590	37,498	43,646	0,180
0,998	22,711	34,790	0,076
0,001	77,909	61,818	0,614
0,920	91,237	64,917	0,167
0,000	75,380	40,772	0,869
0,000	51,605	33,695	0,486
0,826	38,052	41,857	0,140

0,000	73,311	93,148	0,378
0,992	3,506	23,353	0,000
0,082	86,409	47,967	0,320
0,000	82,414	56,647	0,413
0,000	96,154	24,272	0,864
0,000	96,154	24,272	0,864
1,000	0,719	1,241	0,020
0,000	84,587	57,634	0,737
1,000	13,915	13,177	0,058
0,000	83,254	48,221	0,696
0,359	67,171	55,132	0,233
0,999	14,030	21,261	0,105
0,000	92,785	59,013	0,528
0,000	94,211	96,256	0,719
0,944	7,616	24,809	0,000
0,028	45,706	68,563	0,360
0,000	54,963	56,403	0,413
1,000	58,261	5,386	0,101
0,000	86,820	50,313	0,417
0,802	8,115	53,109	0,000
0,000	92,664	NA	0,718
0,000	67,276	74,653	0,617
0,003	34,848	58,514	0,476
0,000	47,259	22,395	0,676
0,266	38,782	60,528	0,247
0,993	5,059	11,848	0,137
0,000	71,276	32,072	0,766
0,045	39,199	62,688	0,330
0,000	51,034	66,334	0,415
1,000	60,999	0,850	0,000
1,000	49,877	1,486	0,175
-	NA	NA	-
1,000	1,509	3,548	0,030

0,278	9,163	NA	0,287
0,000	95,824	97,038	0,967
0,000	81,267	23,451	0,613
0,917	0,527	17,703	0,000
0,987	55,945	8,006	0,185
0,999	63,479	29,228	0,070
0,001	26,003	13,715	0,324
0,000	24,280	20,411	0,458
0,686	43,715	23,011	0,190
0,659	38,661	22,835	0,193
0,000	85,037	75,865	0,758
0,774	9,503	NA	0,111
0,000	97,871	86,794	0,774
0,000	71,402	81,281	0,590
0,997	10,711	17,644	0,048
0,000	50,672	36,833	0,440
0,000	84,872	81,896	0,930
0,000	49,778	82,317	1,003
0,003	36,669	45,083	0,164
0,014	63,155	59,335	0,729
0,960	45,010	10,127	0,157
0,000	71,715	96,510	0,165
0,973	67,583	56,588	0,168
0,366	87,479	64,047	1,443
1,000	71,062	2,307	0,167
0,000	97,350	39,482	0,646
0,000	91,462	95,611	1,730
0,000	16,615	9,404	0,448
0,005	38,376	89,969	0,167
0,526	86,431	68,514	0,167
0,000	70,321	45,973	0,403
0,000	83,314	73,744	0,168
NA	NA	NA	0,976

0,000	84,444	98,485	0,434
0,000	71,984	62,454	0,742
0,000	69,602	13,392	0,284
0,904	22,793	48,397	0,287
1,000	0,115	2,454	0,299
0,625	64,549	21,515	0,730
0,014	23,139	NA	0,507
0,000	93,630	98,368	0,732
0,000	88,609	33,490	0,622
0,000	92,011	94,536	0,301
0,000	74,025	51,417	0,579
0,000	83,841	98,778	0,307
NA	NA	NA	0,315
0,000	64,044	68,974	0,319
0,000	72,593	90,420	0,321
0,961	1,630	14,565	0,324
0,804	88,598	2,424	0,737
0,376	41,339	82,356	1,379
0,981	2,244	22,131	0,120
0,996	36,993	8,710	0,132
0,000	99,638	46,227	0,808
0,989	10,178	46,158	0,142
0,000	99,665	99,247	0,333
0,672	9,630	63,099	0,335
0,354	46,431	51,085	0,337
0,000	99,901	1,193	0,276
0,964	40,664	38,700	0,164
0,984	24,933	19,306	0,341
0,008	95,616	57,713	0,402
0,000	61,800	92,473	0,584
0,237	9,608	15,552	0,646
0,359	55,775	33,206	0,229
0,893	53,476	45,689	0,584

0,000	32,219	19,335	0,588
0,000	62,266	51,105	0,635
0,000	93,827	79,384	0,845
0,828	43,649	67,615	0,956
0,499	41,553	49,208	0,588
0,499	41,553	49,208	0,589
0,499	41,553	49,208	0,207
1,000	16,066	45,709	0,593
1,000	6,030	26,549	1,197
0,967	7,523	30,401	0,637
1,000	3,210	16,999	0,605
0,000	85,064	97,566	0,608
0,037	10,195	40,753	0,609
1,000	34,058	1,075	0,027
0,556	51,852	22,082	0,157
0,488	13,235	8,847	0,613
0,488	13,235	8,847	0,222
0,768	14,903	35,894	0,614
0,000	41,898	71,769	0,617
0,000	99,358	81,447	0,637
0,000	98,667	94,819	0,619
0,000	42,881	70,068	0,638
0,000	99,665	99,247	0,644
0,000	30,261	94,976	0,619
0,000	57,674	76,999	0,622
0,000	65,553	22,659	0,632
0,837	11,989	37,322	0,099
NA	NA	NA	0,197
NA	NA	NA	0,197
0,428	NA	NA	0,197
0,000	79,835	86,637	0,532
0,592	10,667	52,884	0,180
1,000	14,239	4,252	0,537

0,323	62,842	57,937	0,541
0,277	36,071	91,515	0,263
0,000	16,401	NA	1,138
0,000	16,401	NA	1,172
0,081	73,366	60,215	0,542
0,000	88,368	39,335	0,546
0,964	26,250	84,639	0,144
0,923	48,911	23,675	1,336
0,399	32,329	28,416	0,652
1,000	16,949	12,727	0,557
0,000	52,192	55,748	0,608
0,000	15,204	60,978	0,565
0,975	0,477	36,139	0,568
-	NA	NA	-
0,000	92,516	0,235	0,569
0,011	97,289	82,239	0,573
0,007	89,630	99,843	0,371
0,000	69,833	83,206	0,573
0,999	17,388	23,500	0,579
0,005	69,278	53,783	0,307
0,000	89,553	34,976	0,646
0,003	31,737	25,376	0,314
0,000	97,728	69,560	0,655
NA	NA	98,143	0,662
0,013	60,027	32,278	0,423
NA	NA	NA	NA
0,000	41,926	50,792	0,662
0,034	70,063	46,569	0,503
0,658	61,141	66,432	0,482
0,002	59,177	17,820	0,542
0,000	88,016	33,040	1,054
0,000	97,608	90,508	0,483
0,000	34,639	26,647	0,484

0,000	89,739	73,128	0,492
0,158	26,497	3,470	0,492
0,992	23,764	20,802	0,087
-	NA	NA	-
0,992	83,380	56,862	0,502
0,985	6,063	4,233	0,503
0,000	62,140	38,006	0,519
0,000	87,188	92,317	1,277
0,982	22,502	30,938	0,663
1,000	10,645	15,308	0,523
0,997	13,591	33,861	0,047
0,000	40,691	48,534	0,665
0,000	31,298	64,350	0,900
1,000	29,948	19,592	0,657
1,000	10,892	29,238	0,024
0,226	45,432	16,960	0,239
0,000	69,021	50,978	0,684
0,006	22,716	65,220	0,523
0,106	61,377	6,051	0,523
0,000	86,189	69,306	3,202
0,000	64,900	86,755	0,528
-	NA	NA	-
0,878	45,015	43,734	0,091
0,000	57,772	0,694	0,497
0,979	54,601	77,116	0,528
0,000	95,918	99,883	0,688
0,000	41,663	32,659	0,657
-	NA	NA	-
1,000	23,962	0,186	0,719
0,000	75,605	90,860	0,368
0,003	60,362	79,511	1,028
0,184	2,557	NA	0,712
0,000	93,630	98,368	0,712

0,161	60,735	42,141	0,730
0,000	38,798	22,805	0,371
0,008	50,299	NA	0,378
0,000	64,812	93,353	0,341
1,000	1,811	5,562	0,344
0,999	19,550	1,593	0,357
0,910	9,827	22,933	0,145
NA	NA	NA	NA
0,000	93,942	99,521	0,357
0,000	81,317	29,717	0,381
0,999	28,466	23,284	0,358
0,000	46,266	84,418	1,856
0,001	77,690	56,794	0,719
0,934	63,139	76,452	0,360
0,923	5,619	18,182	0,000
0,018	10,925	32,199	0,365
-	NA	NA	-
0,022	60,291	43,695	0,366
0,000	64,982	24,399	0,367
0,996	22,129	11,085	0,368
0,986	38,409	77,683	0,000
0,999	19,418	3,773	0,120
0,058	47,841	46,354	0,414
NA	NA	NA	NA
0,000	88,730	74,115	0,911
0,000	86,129	60,029	0,711
0,000	47,259	22,395	0,676
0,000	54,151	46,911	0,475
1,000	13,421	21,124	0,037
1,000	14,239	4,252	0,111
0,715	19,265	20,850	0,159
-	NA	NA	-
0,000	1,257	0,029	0,284

0,377	29,778	39,267	0,227
0,000	62,491	56,109	0,657
0,922	13,767	40,166	0,081
0,965	13,158	33,030	0,069
0,020	79,413	96,149	0,345
NA	NA	NA	NA
0,000	43,374	61,212	0,453
0,000	52,373	55,484	0,602
0,293	34,464	62,053	0,235
0,512	38,107	31,613	0,169
0,000	45,125	58,925	0,769
NA	NA	NA	NA
1,000	31,111	14,350	0,041
1,000	0,379	4,340	0,235
0,000	61,163	72,502	0,235
0,511	40,911	46,207	0,235
0,008	46,985	53,294	0,404
0,928	57,986	60,127	0,236
0,000	88,027	13,695	1,067
NA	NA	0,313	0,239
-	NA	NA	-
0,000	70,244	38,993	0,523
0,985	38,722	29,296	0,251
0,000	69,053	79,120	0,251
0,925	7,407	56,354	0,756
0,802	77,772	79,003	0,164
0,000	99,276	59,638	0,758
0,000	71,111	89,286	0,263
0,000	71,111	89,286	0,614
0,000	97,674	98,055	0,685
0,000	79,045	66,843	0,263
0,936	4,538	13,148	0,266
0,057	92,543	85,171	0,595

0,000	48,856	97,155	0,759
0,040	91,144	21,300	0,272
0,009	44,219	17,410	0,395
0,000	55,385	59,453	0,778
0,054	77,728	85,709	0,276
0,001	72,346	60,166	0,366
0,000	8,582	14,976	0,276
1,000	16,000	7,263	0,282
0,000	99,868	99,707	0,608